AD-A147 636 THE EFFECTS OF SOIL MOISTURE ON BISTATIC CLUTTER POWER 1/1
(U) ROME AIR DEVELOPMENT CENTER GRIFFISS AFB NY
J F LENNON ET AL. JUL 84 RADC-TR-84-164

UNCLASSIFIED F/G 17/9 NL

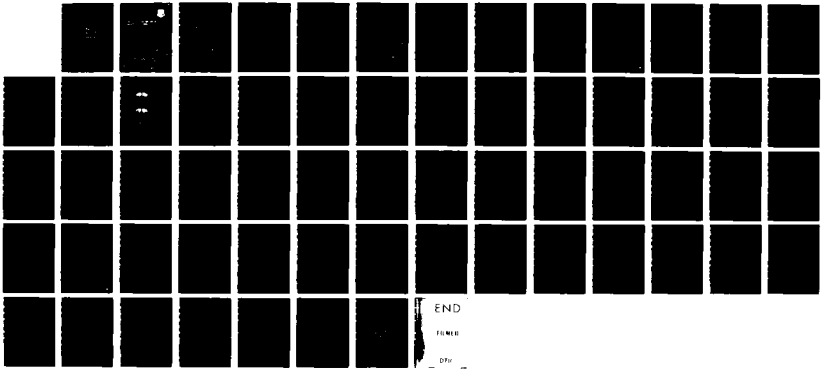

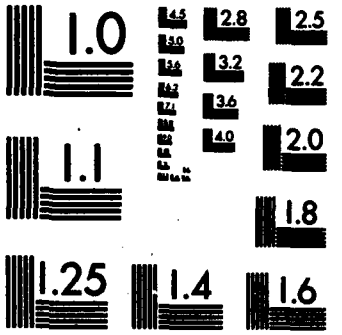

RADC-TR-84-164
In-House Report
July 1984

THE EFFECTS OF SOIL MOISTURE ON BISTATIC CLUTTER POWER

John F. Lennon
Robert J. Papa

ROME AIR DEVELOPMENT CENTER
Air Force Systems Command
Griffiss Air Force Base, NY 13441

This report has been reviewed by the RADC Public Affairs Office (PA) and is releasable to the National Technical Information Service (NTIS). At NTIS it will be releasable to the general public, including foreign nations.

RADC-TR-84-164 has been reviewed and is approved for publication.

APPROVED: Phillipp Blacksmith

PHILLIP BLACKSMITH
Chief, EM Techniques Branch
Electromagnetic Sciences Division

APPROVED: Allan C. Schell

ALLAN C. SCHELL
Chief, Electromagnetic Sciences Division

FOR THE COMMANDER: John A. Ritz

JOHN A. RITZ
Acting Chief, Plans Office

If your address has changed or if you wish to be removed from the RADC mailing list, or if the addressee is no longer employed by your organization, please notify RADC (EECT) Hanscom AFB MA 01731. This will assist us in maintaining a current mailing list.

Do not return copies of this report unless contractual obligations or notices on a specific document requires that it be returned.

Unclassified

SECURITY CLASSIFICATION OF THIS PAGE

REPORT DOCUMENTATION PAGE

1a. REPORT SECURITY CLASSIFICATION Unclassified	1b. RESTRICTIVE MARKINGS N/A
2a. SECURITY CLASSIFICATION AUTHORITY N/A	3. DISTRIBUTION/AVAILABILITY OF REPORT Approved for public release: Distribution unlimited.
2b. DECLASSIFICATION/DOWNGRADING SCHEDULE N/A	
4. PERFORMING ORGANIZATION REPORT NUMBER(S) RADC-TR-84-164	5. MONITORING ORGANIZATION REPORT NUMBER(S)
6a. NAME OF PERFORMING ORGANIZATION Rome Air Development Center 6b. OFFICE SYMBOL (If applicable) EECT	7a. NAME OF MONITORING ORGANIZATION ROME AIR DEVELOPMENT CENTER (EECT)
6c. ADDRESS (City, State and ZIP Code) Hanscom AFB Massachusetts 01731	7b. ADDRESS (City, State and ZIP Code) HANSCOM AFB, MA 01731
8a. NAME OF FUNDING/SPONSORING ORGANIZATION ROME AIR DEVELOPMENT CENTER 8b. OFFICE SYMBOL (If applicable) EECT	9. PROCUREMENT INSTRUMENT IDENTIFICATION NUMBER N/A
8c. ADDRESS (City, State and ZIP Code) HANSCOM AFB, MA 01731	10. SOURCE OF FUNDING NOS. PROGRAM ELEMENT NO.: 61102F PROJECT NO.: 2305 TASK NO.: J4 WORK UNIT NO.: 07
11. TITLE (Include Security Classification) The Effects of Soil Moisture on Bistatic Clutter Power	
12. PERSONAL AUTHOR(S) John F. Lennon and Robert J. Papa	
13a. TYPE OF REPORT In-House 13b. TIME COVERED FROM Jun 82 TO Jun 84	14. DATE OF REPORT (Yr., Mo., Day) 1984 July 15. PAGE COUNT 61
16. SUPPLEMENTARY NOTATION N/A	

17. COSATI CODES			18. SUBJECT TERMS (Continue on reverse if necessary and identify by block number)
FIELD	GROUP	SUB. GR.	Rough surface scattering, Dielectric constants, Electromagnetics, Moisture content
	2014	1709	
	0903		

19. ABSTRACT (Continue on reverse if necessary and identify by block number)

A major question for rough surface scattering analyses is how moisture affects the results. This study represents an extensive discussion of moisture effects in bistatic scattering. Considerable emphasis is placed on the roughness dependence of the effects. Comparisons are presented that show that the standard simplified bistatic model tends to suppress some of the effects and differs considerably from a more complete analysis. The effects of successively increasing the relative moisture levels are shown. A number of antenna power patterns are considered and the effects of relative heights and separation of the antennas are discussed. Finally, the basic study is extended to other system parameters. These include signal frequency and polarization. The relative effect of the moisture is found to be sensitive to these factors and, particularly, to the surface roughness. Originator-supplied keywords include: Electromagnetics, Moisture Content, and Dielectric constants.

20. DISTRIBUTION/AVAILABILITY OF ABSTRACT UNCLASSIFIED/UNLIMITED ☐ SAME AS RPT. ☒ DTIC USERS ☐	21. ABSTRACT SECURITY CLASSIFICATION Unclassified
22a. NAME OF RESPONSIBLE INDIVIDUAL Robert J. Papa	22b. TELEPHONE NUMBER (Include Area Code) (617)861-3735 22c. OFFICE SYMBOL EECT

DD FORM 1473, 83 APR EDITION OF 1 JAN 73 IS OBSOLETE.

Unclassified

SECURITY CLASSIFICATION OF THIS PAGE

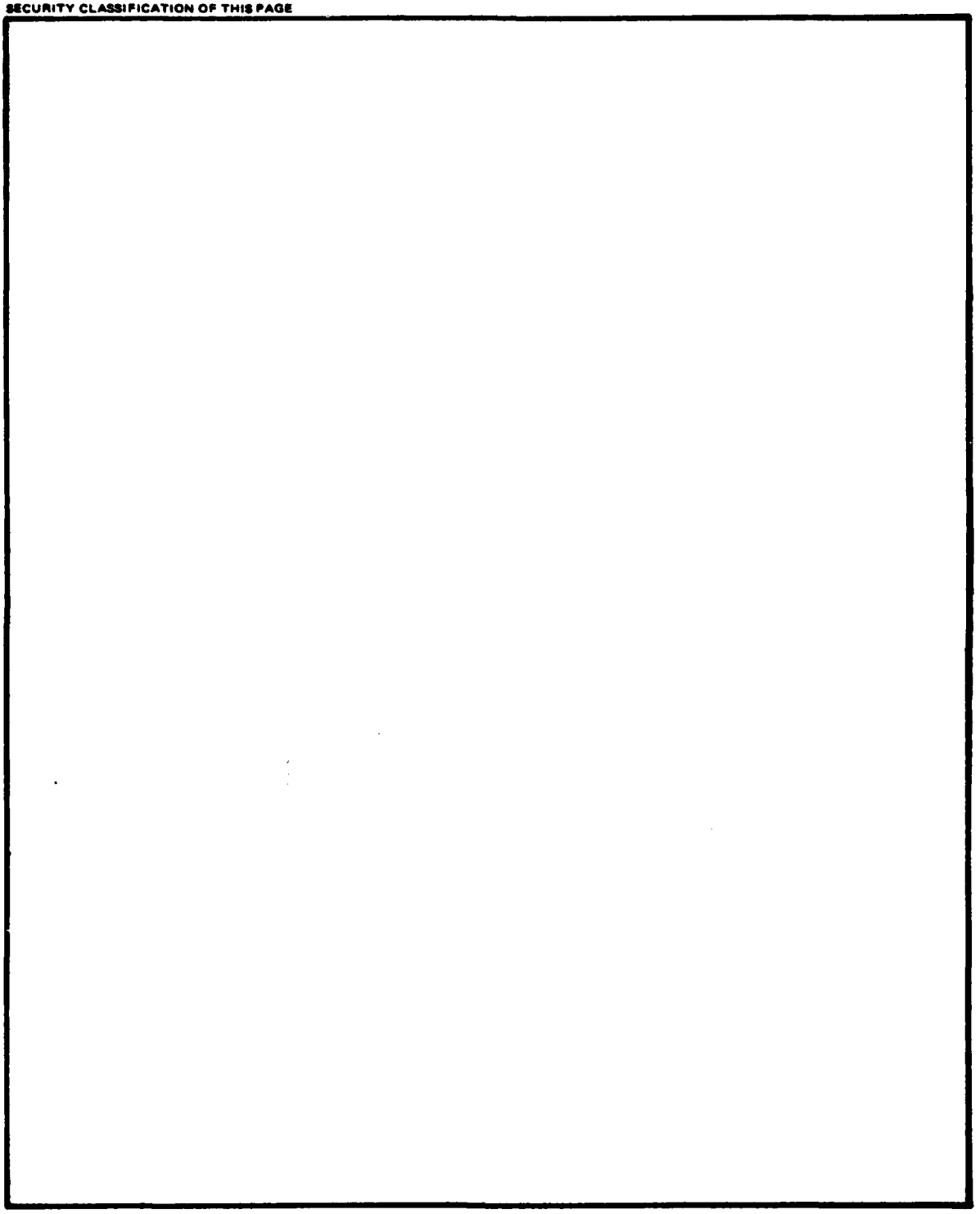

Preface

The authors wish to acknowledge the contributions of Ms. Nancy Kerwin (ARCON) who is responsible for the computer programming aspects that provided the results used in the many comparisons included in this study.

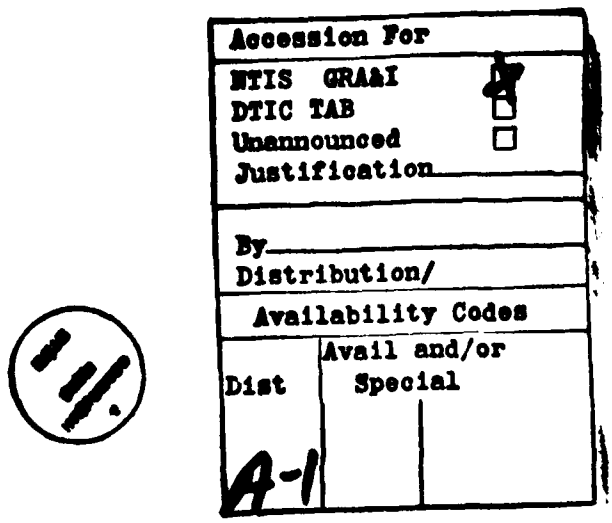

Contents

Contents

Illustrations

Illustrations

Tables

The Effects of Soil Moisture on Bistatic Clutter Power

1. INTRODUCTION

In a number of earlier reports[1-4] we have addressed the question of the determination of electromagnetic scattering from rough surfaces. In these studies the surface has been characterized by a set or sets of descriptive parameters including surface roughness and dielectric constant. Our primary concern has been to establish when the standard Beckmann and Spizzichino[5] definition of "glistening" (scattering) surface combined with an azimuthally independent scattering formulation is an adequate model of the scattering and, conversely, when a more comprehensive model is required. In many instances, significant amounts of incoherent scattered power can be received from areas excluded by the conventional definition.[6] The assumption of azimuthal independence of the scattering cross section (σ°) in the standard model adds to the differences between its results and the more exact case where σ° is considered to vary with azimuthal angle.[7] Consideration of these aspects led us to speculate as to how differences in other factors such as the soil moisture levels would affect the scattering results. In this report we address that question. We are concerned primarily with the relationship between surface roughness and the effects of moisture on electromagnetic scattering in a bistatic

(Received for publication 27 July 1984)

(Due to the large number of references cited above, they will not be listed here. See References, page 41.)

geometry for a wide range of system conditions. These include signal frequency, polarization, antenna pattern, and relative antenna heights. Some considerations relating to the use of different scattering models are included. The interactions are complex so the results will be presented in a format where each parameter is examined in succession. The variation of the moisture effects as a function of roughness is presented for each case.

2. THE ANALYTICAL MODELS

Before presenting the results we will give a brief description of the theoretical models used in the analyses. Then we discuss the introduction of moisture.

2.1 Scattering Models

Models for electromagnetic wave scattering from rough surfaces have been described in considerable detail in the earlier studies.[1-4, 7] For the present report only some significant features will be reviewed, particularly those relating to the differences in the results. The details are given in Appendix A.

The basic models represent a bistatic geometry in which the signal from a transmitter is scattered by a rough surface into a receiving antenna. A conceptual representation is shown in Figure 1. The models are constructed under physical optics assumptions. In these models the normalized scattering cross section of the surface (Ruck et al[8]) includes an appropriate surface dielectric constant. Except where indicated, the signal is vertically polarized. L band and S band frequencies are employed. Several antenna power patterns have been examined. The surface heights are assumed to be described by a bivariate exponential distribution, with a negligible mean surface height. Additional system parameters are shown in Table 1. In this study we will discuss only the diffusely scattered power.

In order to introduce the moisture aspects into the analysis, the surface contributing to the scattering has to be defined. In Appendix A the azimuthal variation of the surface scattering cross section and its effects on the diffuse power have been introduced. In the introduction we indicated how in earlier work we used the related concept of a glistening surface over which the cross section is assumed to be azimuthally independent. Subsequent analysis of this concept resulted in the establishment of limitations that apply to this standard approach.[9] We will discuss how that

8. Ruck, G.T., Barrick, D.E., Stuart, W.D., and Krichbaum, C.K. (1970) Radar Cross Section Handbook, Vol. 2, Plenum Press, New York.

9. Papa, R.J., Lennon, J.F., and Taylor, R.L. (1984) The Use of the Glistening Surface Concept in Rough Surface Scattering, RADC-TR-84-159.

model is affected by changes in moisture level and how its results differ from the general model. Details of this model and its difference from the general model are included in Appendix B.

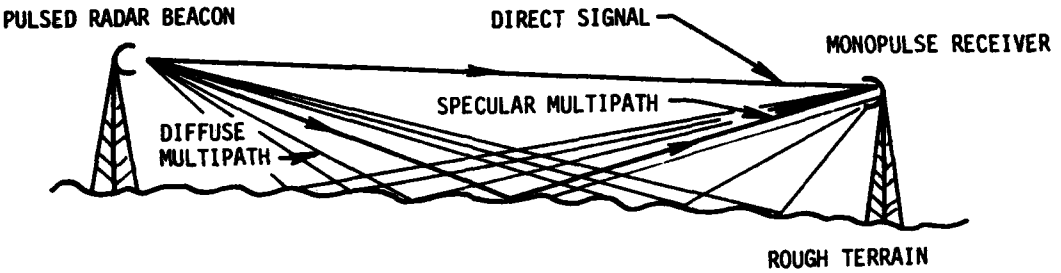

Figure 1. Rough Surface Scattering in a Typical Bistatic Geometry

Table 1. Parameters of the Bistatic System

Front end receiver noise figure	3 dB
Gain of monopulse receiver (sum pattern) antenna	22.5 dB
Gain of transmitter antenna	4 dB
*Height of receiver antenna	1220 m
*Height of transmitter antenna	100 m
*Signal polarization	vertical
Peak transmitter power	350 W
Pulse length	20 μ sec
*Azimuthal beamwidth (receiver)	3°
*Wavelength	0.275 m
Transmission line loss factor	3 dB
System processing loss	2 dB
Normalized pattern slope	1.5

*Indicates a parameter that was varied for some cases in this study.

2.2 Moisture Aspects

As indicated previously, the moisture variation is introduced into the models by changing the value for the dielectric constant appropriately. In the early work,[1-4] we assigned dielectric constants for the terrain as described by the geologic coding of the data base. When we turned to the question of glistening surface limitations,[6] we used both the data base values and a number of cases where the entire surface was assumed to be of uniform roughness and to be cultivated terrain with complex dielectric constant, $\epsilon_r = 80 + j\,9.0$.

In this present analysis, we use three soil descriptors reflecting different moisture levels and consider how the relative roughness affects the scattering.[10] For dry desert type sandy soil we used

$$\epsilon_r(1) = 2 + j\,1.62 .$$

For ordinary dry ground,

$$\epsilon_r(2) = 4 + j\,0.006 .$$

Finally, for moist soil,

$$\epsilon_r(3) = 30 + j\,0.6 .$$

These are the basic values for the study. In the instance where the different aspects of the dielectric constant are investigated, additional values are used but these do not necessarily correspond to physically meaningful surface conditions. Further discussion of the complex dielectric constant will be given in Section 3.1.3, but some basic factors are worth noting here.

The complex dielectric constant of a surface consists of two parts which are describable in term of the surface permittivity, K, and its conductivity, σ. Thus, $\epsilon_r = K/\epsilon_o - j\sigma/\omega\epsilon_o = \epsilon_1 - j\epsilon_2$ where ϵ_o is the dielectric constant of free space, f is the radar frequency, and $\omega = 2\pi f$.

Kerr[11] discusses the relative behavior of the two terms of the relative dielectric constant for land types. For land surfaces both ϵ_1 and ϵ_2 are in general much lower than for water. For dry soil the value of ϵ_1 can be as low as 2 but is more likely to lie in the range from 3 or 4 to 20. Small values of ϵ_2 tend to occur simultaneously with low values of ϵ_1 for dry, rocky, or sandy soil whereas higher values of both tend to occur for rich, fertile soils.

---

10. Long, N.W. (1975) Radar Reflectivity of Land and Sea, Lexington Books.
11. Kerr, D.E. (1951) Propagation of Short Radio Waves, McGraw-Hill, New York.

Amplitude and phase changes in Fresnel reflection coefficient have been plotted as a function of grazing angle for various frequencies.[12] Meeks[13] shows the effect of increasing moisture content on the Fresnel reflection coefficient as a function of grazing angle at 8 GHz. He indicates that for both polarizations the effect is less significant at small angle and the horizontal results there are far less variable than the vertical ones. Also, the relative magnitude of the moisture curves is reversed below about 10° while above that the behavior is similar for the two polarizations. The carryover of these factors into the present analysis will be interesting to observe. His values for ϵ_r as a function of moisture and frequency are based on results of Njoku and Kong.[14] They indicate that ϵ_1 is essentially independent of frequency until moisture levels of above 20 percent are reached, at which point the water introduces frequency effects.

We now turn to the discussion of the results that were generated. These results show that there is no simple conclusion about moisture. The effects turn out to be highly dependent on the conditions of interest.

3. RESULTS

The results show the effect of moisture on rough surface scattering for several different sets of system parameters and emphasize that the magnitude of the effect is highly dependent on the level of roughness. In each section we introduce the aspect being addressed by considering the variation as a function of antenna separation for a limited set of roughness conditions. This relates the material to earlier studies that we have performed.[1-4] Then, results are presented showing the effect of moisture on scattering as a function of roughness for each particular set of conditions.

3.1 Scattering Model

In this initial section we want to address several basic concepts. The first is to establish the baseline results for our study of the dependence on surface roughness. Next, we show how use of a simplified model alters the initial results. Finally, we examine a systematic variation in moisture content and the resultant effects on the scattering.

---

12. David, P., and Voge, J. (1969) Propagation of Waves, Pergamon Press, Oxford.
13. Meeks, M. L. (1982) Radar Propagation at Low Altitudes, Artech House, Dedham.
14. Njoku, E. G., and Kong, J. A. (1977) Theory for passive microwave remote sensing of near surface soil moisture, J. Geophys. Res. 82:3108-3118.

For these comparisons the antenna patterns of Figure 2 are assigned to the receiver and the transmitter is assumed to have an isotropic antenna power pattern. The parameters of Table 1 apply. The results with the general scattering model are identified as being for the full integration surface. The simplified model results are referred to as standard surface results.

3.1.1 INTRODUCTION

The initial results address the topic of continuously varying the separation for a given roughness level. This corresponds to the results that would occur if the receiver were approaching the transmitter along a fixed trajectory and scattering calculations were made at successive stationary positions.

Figure 3 shows the diffuse scattered power received at a fixed antanna as the receiver is moved along a straight line path approaching the transmitter. The full scattering surface is considered in this case. These results do not include the shadowing correction factor. The three moisture conditions are depicted for each roughness level.

In Figure 3 several trends can be seen. Here, the degree of roughness is inversely proportional to T. As the surface roughness decreases, for a given moisture factor, there is an increase in the relative difference between the peak power for small distances and that for large separations. Next, the sequence of curves shows a peak in magnitude at the intermediate roughness level (T = 100 m). Then, we can see the effect of moisture content becomes more significant as the surface becomes smoother. In these cases the basic result is that the normal and sandy surface results are almost equivalent while the moist results are quite distinct at all separations; this does not hold true in the case with the largest slopes for which all three curves are close beyond a separation of 30 NMi. The relative magnitudes of the three moisture level curves remain of the same order across the entire range of surface roughness conditions.

As was discussed in Papa et al,[6] the diffuse power is a function of σ/T. Thus, we might expect that the corresponding moisture effects are equivalent for the same σ/T ratio. This is shown in Figure 4 which contains results for the general surface assumption for two sets of conditions with approximately the same σ/T ratio, 0.05. Indeed, a look at Figure 3, where the related case $\sigma/T \sim 0.03$ is shown, indicates quite similar behavior in that instance as well. This introduces the concept of considering the moisture effects as a function of surface roughness (σ/T) and this generalization will be examined in detail in the following section.

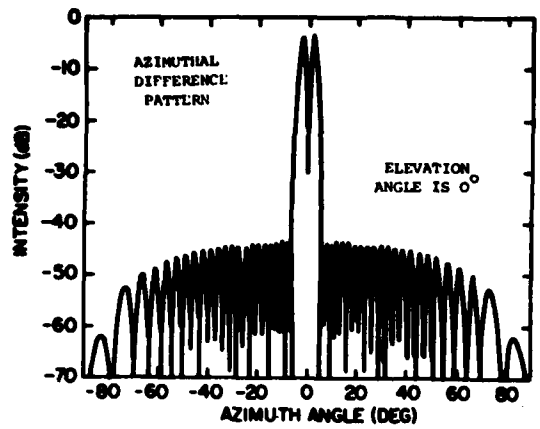

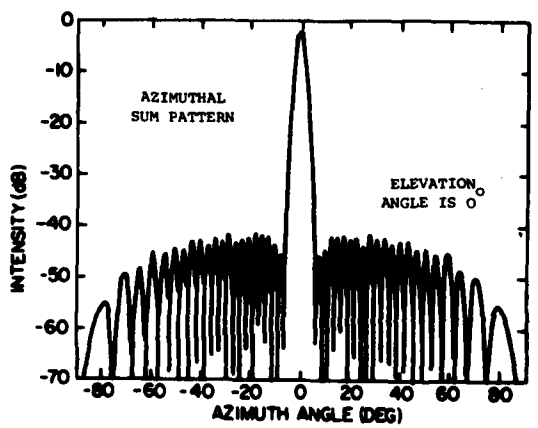

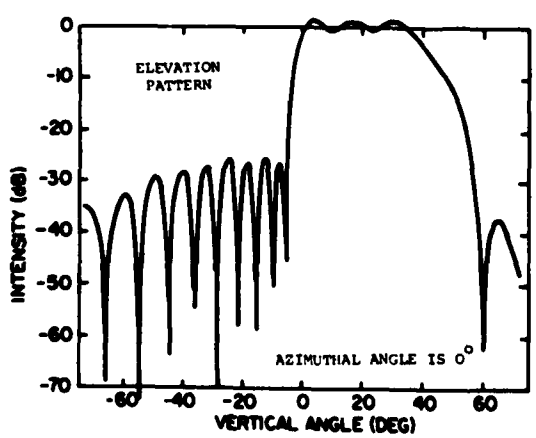

Figure 2. Azimuthal Monopulse Sum and Difference Power Patterns and Elevation Power Pattern for the Receive Antenna

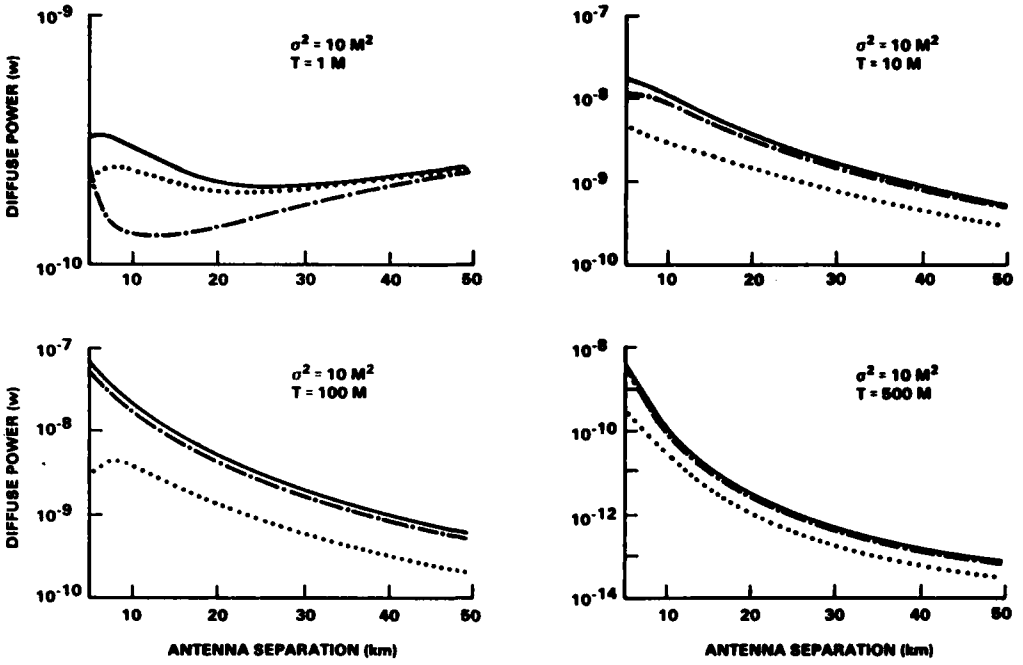

Figure 3. Diffuse Power vs Antenna Separation, Full Surface Solution Without σ^2 = 10 M^2, T = 1, 10, 100, 500 M: ——— ϵ = (2, 1.6), . _ . _ ϵ = (4, 0.006), and .... ϵ = (30, 0.6)

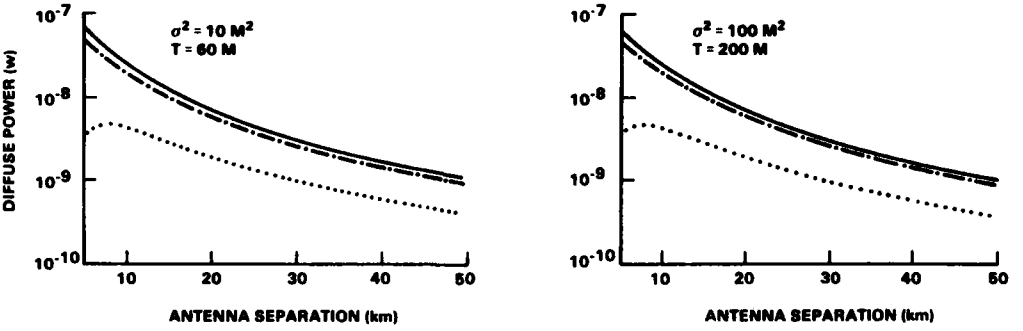

Figure 4. Diffuse Power vs Antenna Separation, Full Surface Solution Without Shadowing σ/T = 10 M^2; σ^2 = 10 M^2, T = 60 M and σ^2 = 100 M^2, T = 200 M: ——— ϵ = (2, 1.6), . _ . _ ϵ = (4, 0.006), and .... ϵ = (30, 0.6)

In that section we will summarize the variation of moisture effects as a function of roughness for the basic set of parameters. Two soil conditions are presented, sandy and moist, and three antenna separations are examined. The surface heights are assumed to have an exponential distribution but this is not critical as was shown in Papa et al.[9] The effect of shadowing is included. The difference in behavior that appear when the simplified model is used are shown. Only a summary is presented here, the detailed comparison of the differences for the two models and the relative effects of shadowing are contained in Appendix C.

3.1.2 COMPARISONS

The appropriate cases are summarized in Figure 5. This shows the shadowed diffuse power as a function of roughness and separation for both surface moisture conditions and both scattering area definitions. The comparison of the overall results for the two of scattering models shows a number of distinctive patterns. First, the full integration peak power exceeds the usual integration surface levels by about two orders of magnitude. Second, for all cases the dry soil results exceed the moist soil ones except at large σ/T values. Next, the 5 NMi usual integration case shows anomalous behavior in relation to the other cases. The 30 NMi and 50 NMi standard surface cases peak at smoother surface conditions ($\sigma/T \sim 0.02$) than corresponding cases where the entire surface is included (peak at $\sigma/T \sim 0.05$).

The oscillations in the moist surface curves for the standard surface are not present when the full surface is integrated. This aspect is examined in detail in Appendix C. This effect may be due to the fact that there are no restrictions on the values of σ/T for the full integration surface to be valid, whereas there are the upper limit restrictions on the values of σ/T for the standard surface.

The difficulty with this explanation is that the slope variations are moisture related and do not appear for the sandy soil cases. This aspect is explored again in Appendix C. Thus, this simple explanation is not sufficient by itself and any rationale for a relationship between dielectric constants and the effect of violating roughness constraints is not at all evident.

The case of 5 NMi requires particular attention. The first point to note is that, at this separation, the Beckmann and Spizzichino definition for the limits of glistening surface results in the disappearance of any such surface (difficulty with the assumption of parallelism) at small σ/T values as well as a general lessening in surface extent even at larger values. For these conditions the moist surface results, in particular, are different in that they reach a peak at $\sigma/T \sim 1.0$. The dry surface shadowed power curve also has a delayed peak in comparison to other separations. The full integration case is somewhat different. For the dry surface the peak power occurs at the same roughness level as that of the other separations.

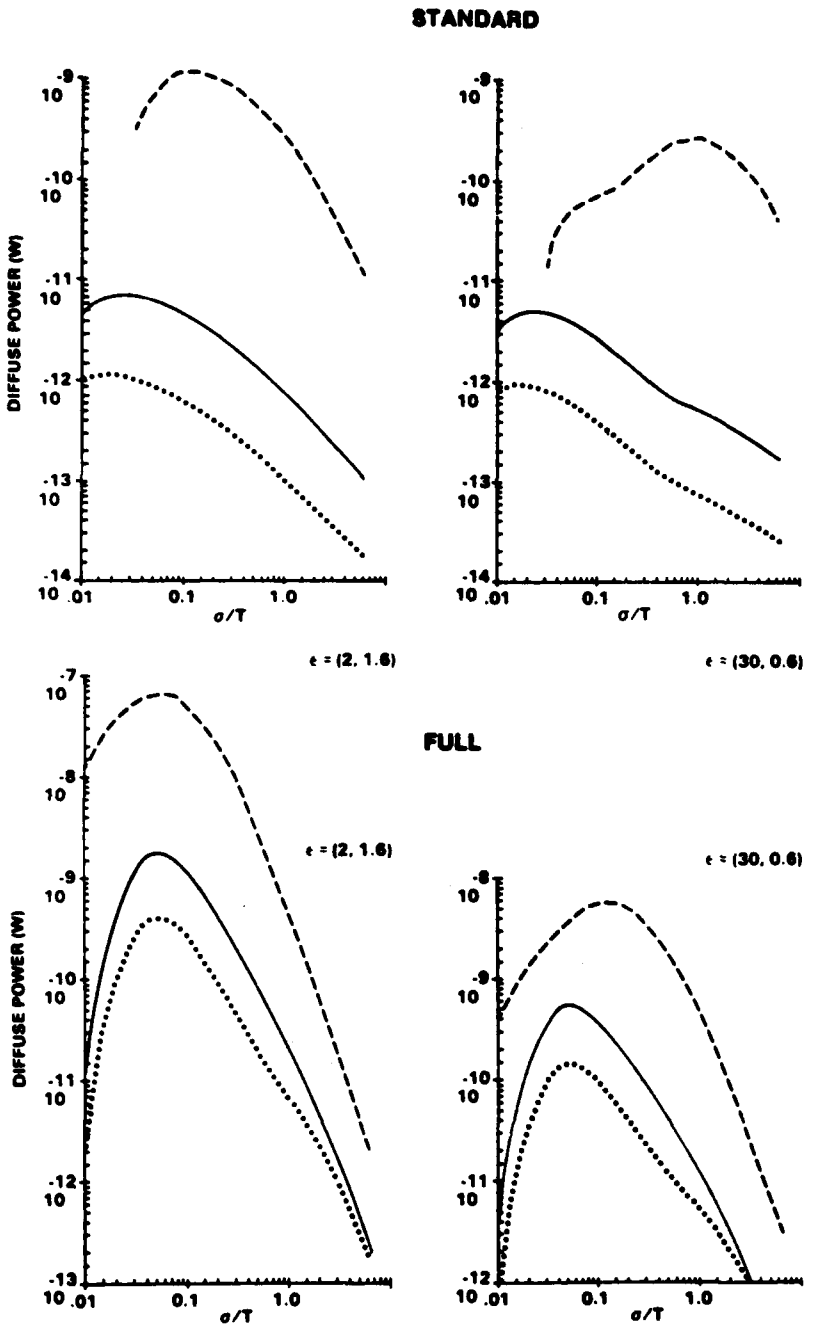

Figure 5. Diffuse Power vs Roughness for Both Models With Shadowing and ϵ = (2, 1.6) and ϵ = (30, 0.6): ___ 5 NMi, —— 30 NMi, and .... 50 NMi

The moist surface, though, peaks at a slightly rougher slope condition at 5 NMi than does the dry case although at other separations both occur at the same point. The end result of these disparate trends at 5 NMi is that the amount of power not included in the usual integration results as compared to the full integration cases is quite variable as a function of roughness while at 30 NMi and 50 NMi the peak power tends to apply in general.

The wide range of differences in the two sets of results, the large power spread at a given σ/T ratio, the different peak locations, the absence of crossover at 30 NMi for full integration, and the secondary peak at 50 NMi for that case (which is not completely suppressed by shadowing) all serve to show that care must be taken in the determination of the effects of moisture and that use of the standard scattering formalism can lead to serious discrepancies.

3.1.3 SUCCESSIVE MOISTURE LEVELS

Up to this point we have examined the basic roughness dependence of scattered power for a specific set of soil moisture contents and have noticed several differences that are present when the two different scattering models are used. In this section we will extend these initial findings to additional cases and discuss the implications of the results for successively increasing moisture levels.

We begin this study with the results shown in Figure 6. In this figure we show the variation along a trajectory for two roughness levels using the full integration surface definitions (for this comparison, shadowing is not included). For this case, the dielectric part of the complex dielectric coefficient was fixed at either $\epsilon_1 = 4$ or $\epsilon_1 = 30$ and the conductive term ϵ_2 was allowed to vary. At the two roughnesses, the results for $\epsilon_1 = 4$ are greater than those for $\epsilon_1 = 30$. For the same ϵ_1 value, the relative magnitudes are reversed as T varies from 10 m to 100 m. Also, at short ranges the respective curves show some changes in slope. The most significant aspect though is that as ϵ_2 is varied ($0.006 \leqq \epsilon_2 \leqq 1.6$) no significant effect is visible. For $\sigma^2 = 10\ m^2$, T = 10 m, the condition $\epsilon_2 = 60$ was also considered and that was sufficient to produce a decrease in scattered power. Thus, a decrease of ϵ_2 of three orders relative to the ϵ_1 value had no effect while a single order increase was significant. Also, it should be noted that for these conditions the whole range of effects is essentially independent of distance between the antennas. This behavior resulted in our carrying out a more comprehensive study of the effect of varying ϵ_1 or ϵ_2.

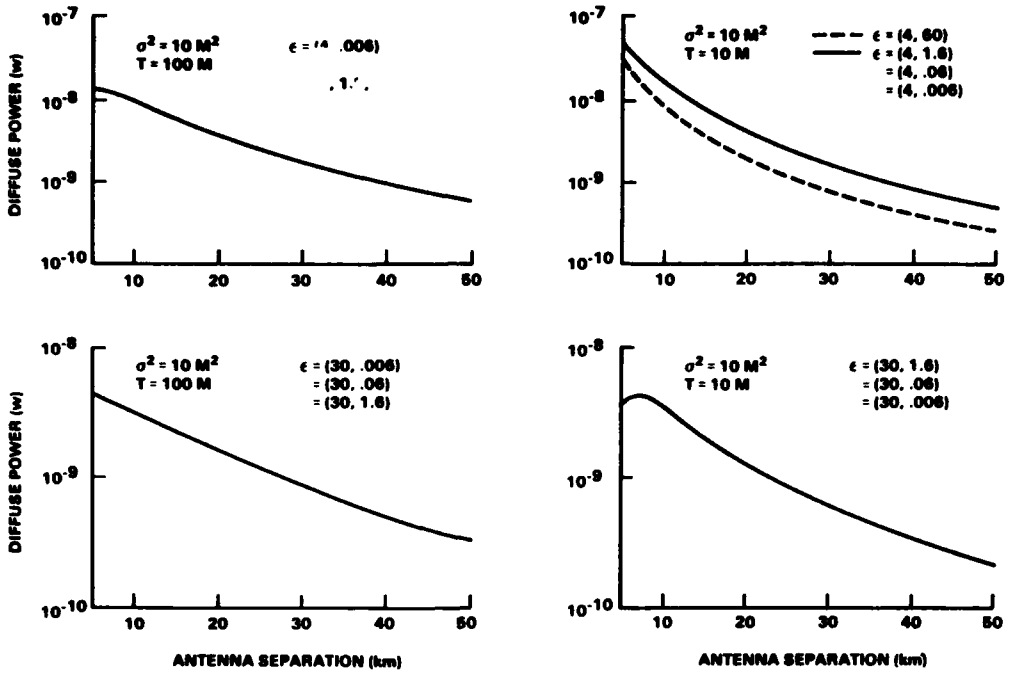

Figure 6. Diffuse Power vs Antenna Separation, Full Surface Model With Different Surface Roughness

The results are summarized in Figure 7. The $\sigma^2 = 10\ m^2$, T = 100 m case used above was repeated for numerous values of ϵ_2 ($\epsilon_1 = 4$) at three different antenna separations. Similar behavior occurred. The power is relatively constant at $\epsilon_2 < 2$ for all distances; then a decrease occurs; this is followed by an increase that exceeds the original level. The change depends on separation. This is consistent with considering the surface as being a lossy dielectric with increasing absorption until it becomes sufficiently reflective that the scattered power is increased. The different transition points for the three distances indicate that the analysis is dependent on the scattering angles associated with the surface even though the results are an integration of the contributions over the entire glistening surface.

The final stage of the examination of the effect of variability in ϵ_r was a sequence of conditions which represented a series of increasing moisture content. The new cases which are in the form of power vs roughness are for the full surface formulation with shadowing. These results are shown in Figure 8. To see the development of moisture effects, this figure should be examined in conjunction with the full integration cases in Figure 5. A correlation can be made between the

dielectric constants of these cases and those for successive moisture percentages indicated in Meeks' book.[13] The connection depends on the point made from Figure 7 that for small imaginary components there is little variation in the results for large changes in the imaginary value. In these terms, the progression ranges from an extremely dry surface, through 10 percent and 20 percent moisture content, and finally to an extremely moist condition.

The concept of model differences for successive moisture levels is pursued in Appendix C. Further comments on the standard surface slope variations are included there also.

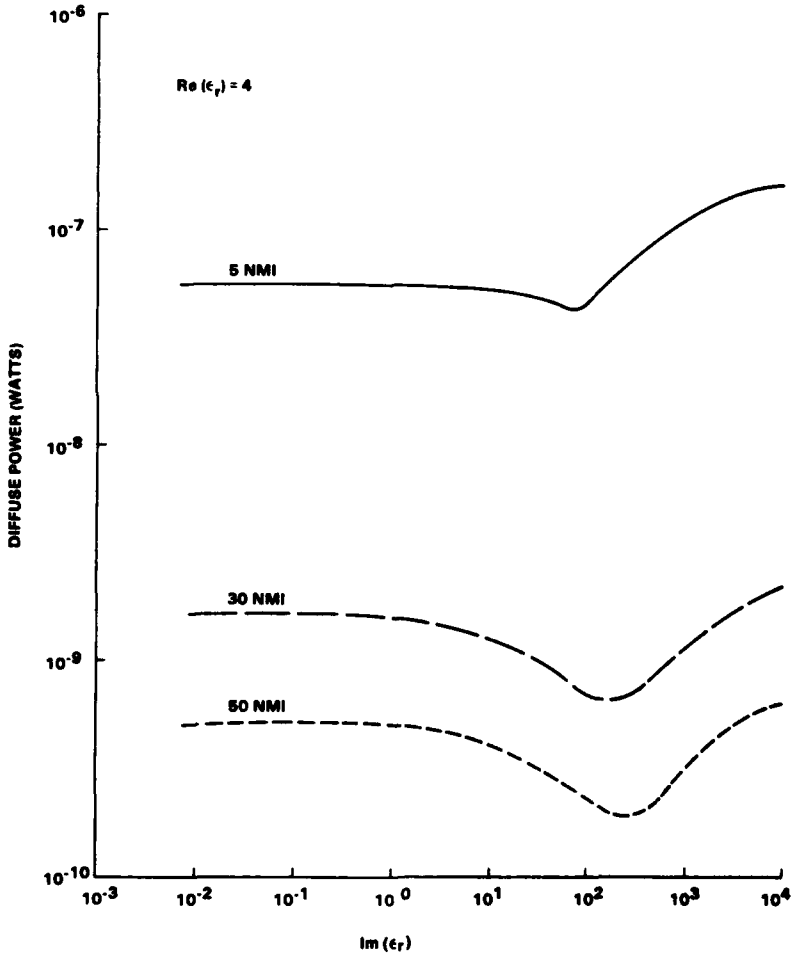

Figure 7. Diffuse Power vs Surface Conductivity, Full Surface Model Without Shadowing σ^2 = 10 M^2, T = 100 M: ____ 5 NMi, — — 30 NMi, and _ _ _ 50 NMi

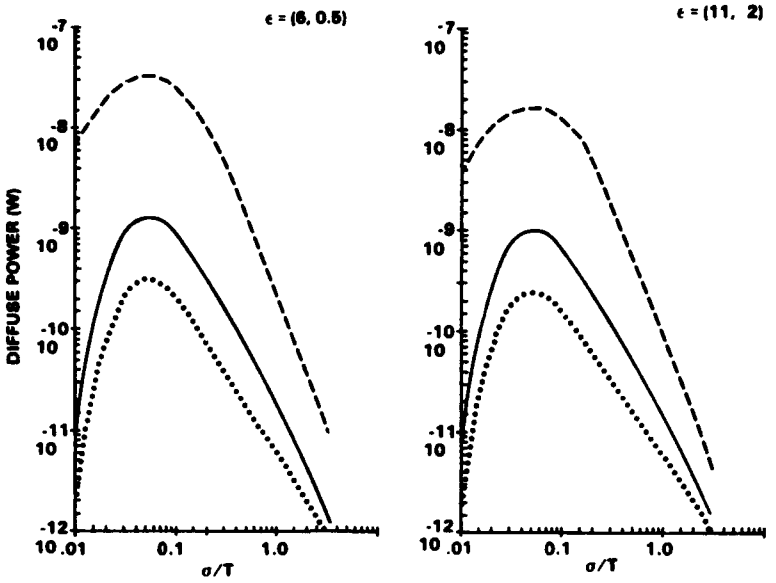

Figure 8. Diffuse Power vs Roughness, Full Surface Model With Shadowing ϵ = (6, 0.5) and, ϵ = (11, 2): _ _ 5 NMi; —— 30 NMi, and ···· 50 NMi

3.2 Antenna Power Pattern

In the previous section we presented a series of results that were obtained using a specific set of system parameters. In this section we will address the question of moisture effects for systems that have alternative antenna power patterns and will examine the roughness dependence for those cases.

One specific aspect of the particular antenna system used in the study of Section 3.1 might suggest that differences in the results are only valid in the one instance. That aspect is the receiving antenna azimuthal power pattern (see Figure 2). The pattern contains a centerline null which removes the centerline σ° contribution from the total diffuse power. The question is whether it is that aspect which allows the azimuthal contributions to dominate the diffuse power result and consequently whether there would be moisture related differences if alternative azimuthal power patterns were considered.

To answer that question the original power pattern was replaced by one having its peak at the centerline with the power remaining at that level over a considerable fraction of the entire pattern. When the diffuse power is calculated for the new power pattern, differences in the moisture behavior can still be seen. A further confirmation was sought by introducing a third power pattern. This case consists in a parabolic pencil beam shape.

3.2.1 INTRODUCTION

Results for each of the three patterns are presented in Figure 9, Figure 10, and Figure 11 for different roughness conditions. The signal is vertically polarized, its wavelength is 0.275 m, and the antennas continue to be at the two different heights. In Figure 9, $\sigma^2 = 10\ m^2$ and T = 10 m; Figure 10 shows the results for $\sigma^2 = 10\ m^2$ and T = 100 m; and Figure 11 has a sequence of varying roughness levels for the surface between the antennas. This last case is representative of actual terrain in eastern Massachusetts.[1] In these three figures the trajectory format is used. For these comparisons the effect of shadowing is excluded. The intent here is not to give a complete roughness study but to verify the effect of the antenna pattern.

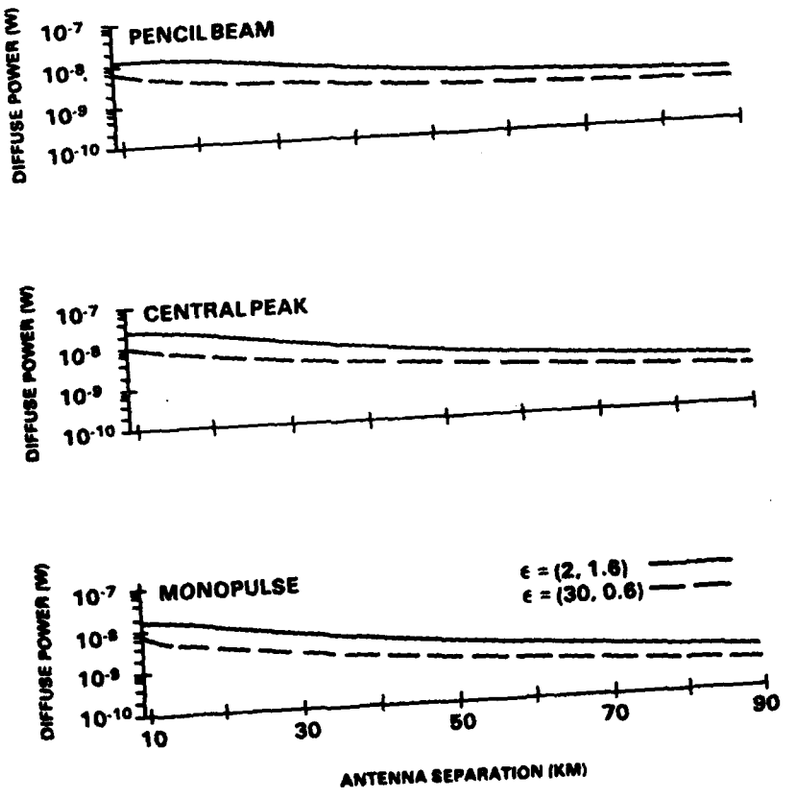

Figure 9. Diffuse Power vs Antenna Separation for Three Antenna Power Patterns, Full Surface Model Without Shadowing and $\sigma/T \approx 0.3$: —— ϵ = (2, 1.6), and —— ϵ = (30, 0.6)

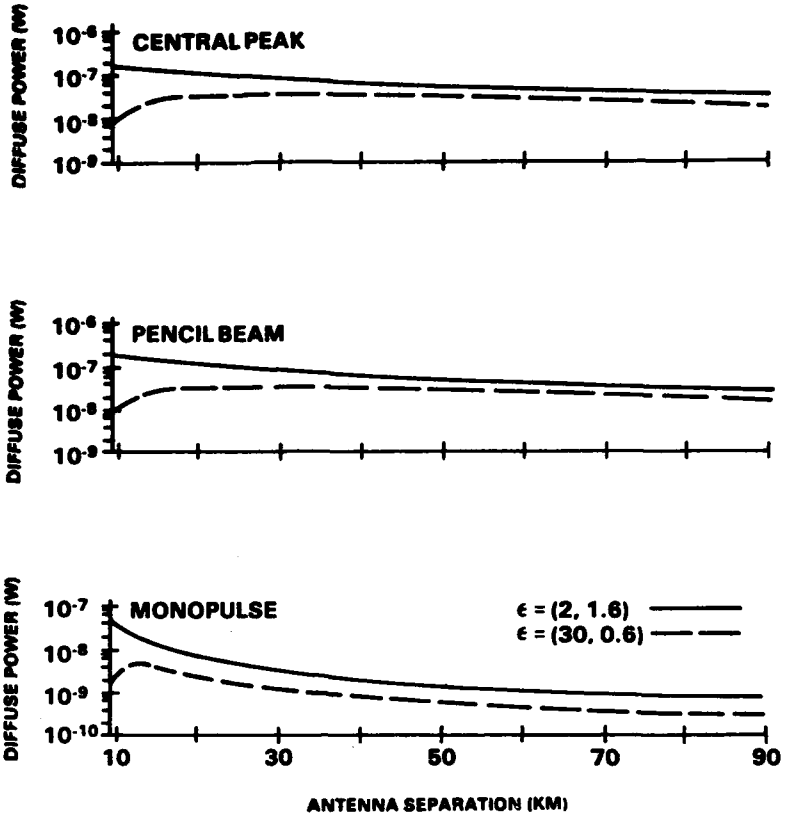

Figure 10. Diffuse Power vs Antenna Separation for Three Antenna Power Patterns, Full Surface Model Without Shadowing and $\sigma/T \approx 0.03$: —— ϵ = (2, 1.6), and — — ϵ = (30, 0.6)

The first point to notice in Figure 9 is that the results for centerline peak (with constant power) pattern and the pencil beam are extremely close, with slightly higher values for the constant power case. This is consistent with the pattern shapes. There is a more rapid decrease in the pencil beam as azimuth is increased but concurrently there is a fall off in the surface contributions away from the centerline so that the results remain similar. Both maximum power and maximum moisture effects occur at small separations but the values are essentially constant over the range of separations. The moisture introduces a decrease in power of about a factor of two. When these results are compared with the monopulse ones we see that the effect of moisture is slightly greater at short distances for the monopulse case and again remains fairly constant (slightly less) over the range of separations. However, the peak power for both soil conditions is always less for

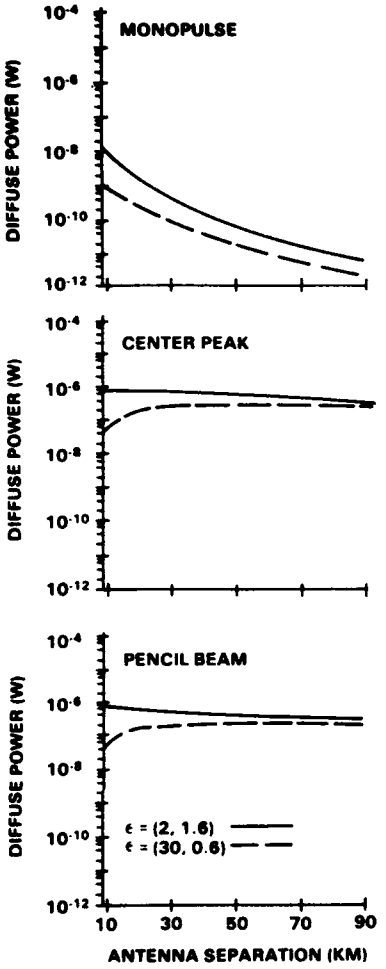

Figure 11. Diffuse Power vs Antenna Separation for Three Antenna Power Patterns, Full Surface Model Without Shadowing and Multiple Roughness Levels: ——— ϵ = (2, 1.6), and — — ϵ = (30, 0.6)

the monopulse case than for the other patterns and shows a considerable fall off with antenna separation. The main point here is that the effect of moisture is present for all three patterns.

In Figure 10 the same three patterns are compared as a function of separation for the two moisture levels but here the surface is slightly smoother than in Figure 9. The overall behavior is quite similar to that of the rougher surface except that the power levels are higher. The pencil beam and centerline peak cases are indistinguishable indicating that off axis contributions fall off more rapidly at this σ/T condition. For all three patterns the effect of moisture is greatest at 5 NMi and beyond a separation of 10 NMi does not appear to be sensitive to the distance. The short distance effect is about a factor of twenty while the longer distances cases differ by about a factor of three. Again, the monopulse has

considerably less diffuse power and shows the decrease with separation that is not true for the other cases. In general, but particularly at short distances, the effect of moisture is greater for this smoother surface.

In Figure 11 the conditions are slightly different than before. Here, instead of fixing the local surface roughness, we replaced the constant surface with a representation of an actual terrain region. This more general case allows multiple roughnesses to be present. The trajectory extends only to 30 NMi, consistent with the extent of the data base used in the calculation. The centerline peak and pencil beam pattern results are again virtually identical. The effect of moisture is greatest at short distances (a factor of 2.5) and decreases with distance. The power levels are only minimally affected by distance. For the monopulse the short distance moisture effects are about the same but the longer distance effects remain more pronounced than for the other patterns. The power level for the monopulse is about two orders of magnitude less at short distances and the decrease with distance is about five orders of magnitude at 30 NMi. In contrast, the presence of centerline power preserves the level of diffuse scattered power at relatively constant levels as a function of separation. Even for this multiple roughness case, effects of moisture can always be seen for all three antenna patterns.

3.2.2 ROUGHNESS EFFECTS

The initial comparisons for antenna pattern effects show the effect of antenna separation for selected roughness levels. The next case stresses the roughness dependence. For this example, the azimuthal power patterns for the two antennas were reversed. The remaining parameters were held fixed. The results are derived using the simplified scattering model. The shadowed curves can be compared with the standard surface results of Figure 5. The combined results for the three distances for this new pattern are shown in Figure 12. Both shadowing and non-shadowing cases are presented. A detailed discussion of the effects of shadowing at the three separations is presented in Appendix C. The analysis there includes a comparison with the corresponding shadowing effects for the original antenna pattern.

Some general comments can be made. For both soils, the crossovers are present for all distances and the shadowed crossovers occur at about the same roughness as the unshadowed. For a given σ/T ratio, the decrease in diffuse power due to shadowing is more pronounced as the separation increases. The peak sandy surface power always exceeds the corresponding moist surface peak and both exceed the corresponding peaks for the original pattern by an order of magnitude. Finally, the unusual slope changes for the moist soil case are present at all three distances and their magnitude is more pronounced for this new antenna pattern.

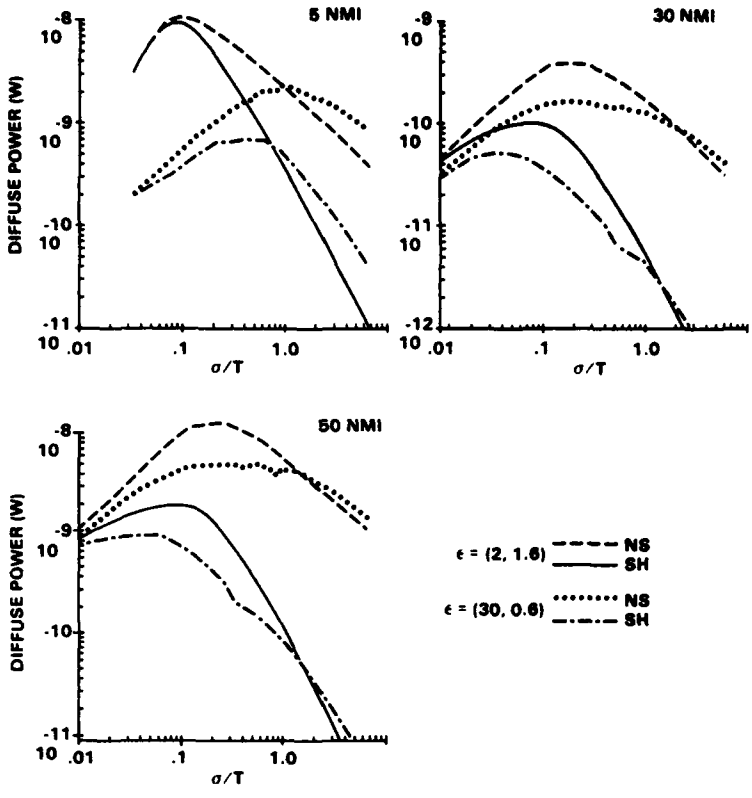

Figure 12. Diffuse Power vs Roughness for Reversed Azimuthal Power Patterns, Standard Surface Model With and Without Shadowing, for ϵ = (2, 1.6) and ϵ = (30, 0.6), at Three Antenna Separations

In summary, the result of introducing new antenna patterns is a wide range of moisture related effects which vary with the features of the particular pattern. Since the behavior is so distinct there is no obvious way to predict just how moisture will affect the scattered power dependence on surface roughness for a particular set of antenna and system parameters.

3.3 Signal Polarization

we have shown how changes in the antenna pattern affected the behavior of the rough surface scattering for different moisture contents. We now return to the original pattern and change the signal polarization. In the initial series of cases the polarization was always vertical. In this section we will examine some results for the scattering when the signal is horizontally polarized. As has been the procedure in previous sections, we will introduce some distance dependent results, Figure 13

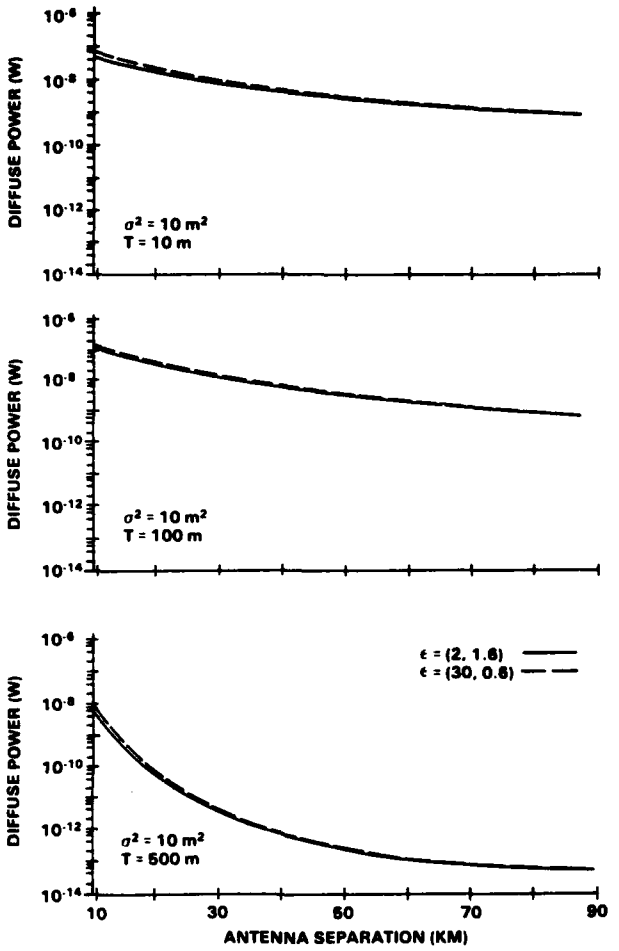

Figure 13. Diffuse Power vs Antenna Separation for a Horizontally Polarized Signal, Full Surface Model Without Shadowing, at Three Roughness Levels: ——. ϵ = (2, 1.6) and — — ϵ (30, 0.6)

for the full integration case. The results do not include shadowing. The cases considered represent $\sigma^2 = 10\ m^2$ and T = 10 m, 100 m, 500 m. Once those trajectory results (without shadowing) have been examined for trends, the final figure in the set is considered. In Figure 14 the full integration results for horizontal polarization, including the effect of shadowing, are presented as a function of the surface roughness. As in the case of antenna pattern variations, the results shown in Figure 13 can be compared with the corresponding trajectory for vertical polarization that were shown in Figure 3 and the results in Figure 14 can be compared with the related ones in Figure 5.

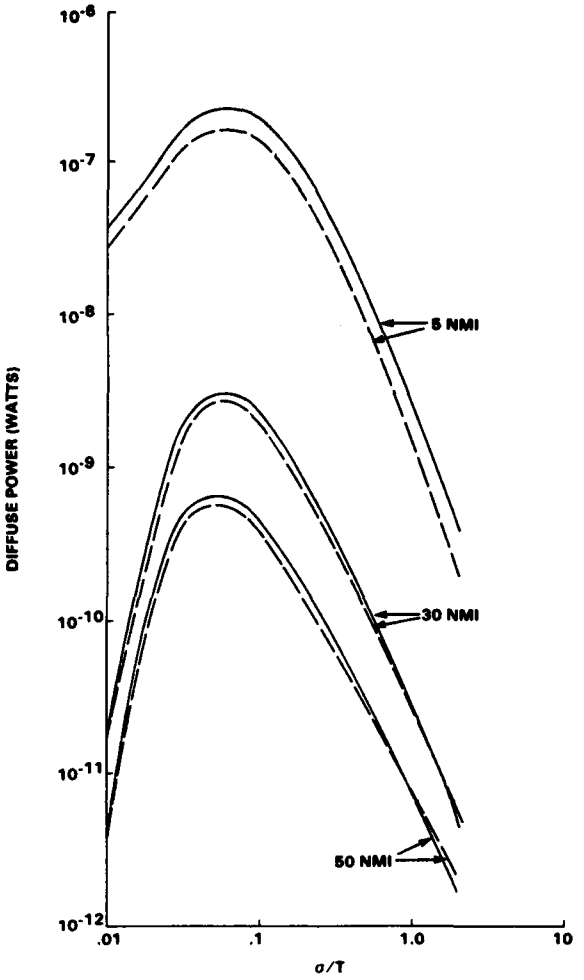

Figure 14. Diffuse Power vs Roughness for a Horizontally Polarized Signal, Full Surface Model With Shadowing, at Three Antenna Separations: ____ ϵ = (2, 1.6) and ——— ϵ = (30, 0.6)

3.3.1 INTRODUCTION

In Figure 13 we see full integration results for a series of progressively rougher surfaces. The smoothest (T = 500 m) shows the most dramatic decrease in power with separation (neglecting shadowing) and over the entire range there is little effect of moisture (the moist soil case is marginally higher). For the T = 100 m case the two soil curves show the highest power levels with the moist soil having slightly more diffuse power than the dry soil. The two curves are much

less affected by separation than the T = 500 m case. For T = 10 m the results are almost identical to those for T = 100 m, except for slightly less diffuse power when the two antennas are close.

If we make comparisons with the corresponding cases of Figure 3 (vertical polarization) we see that in both cases the effects of moisture are relatively insensitive to separation but the effects are greater for vertical polarization. It should be noted that the relative position of the two moisture curves reverses with polarization so that the moist soil power levels are greater than those for dry soil when the signal is horizontally polarized.

These comparisons give some indications of how moisture effects are related to the polarization of the signal and the surface roughness. This aspect will be considered in greater detail in the next discussion.

3.3.2 ROUGHNESS EFFECTS

The most important conclusions about moisture and polarization are to be drawn from the analysis of the roughness dependence plots of Figure 14. Before examining the relationships to the vertical polarization results, we can make some observations about the horizontal scattering at the three distances.

The first observation is that at all separations the scattered power from the moist surface exceeds that from the dry soil except at large σ/T values. The difference is greatest at 5 NMi and there is not much to distinguish between the effects at the other separations. *All three sets* of double peaks occur at about the same roughness $\sigma/T \sim 0.06$. There does not seem to be any sign of crossover at 5 NMi at least as far as the plots were extended while for the remaining distances the crossover occurs at lower σ/T as distance increases.

The comparisons with the full surface vertical polarization results with shadowing in Figure 5 are quite interesting. First, the effect of moisture at a given separation is much more pronounced in the vertical polarization mode than in the horizontal one. Second, we see that, in general, the moist surface results exceed the dry surface ones for the horizontal case, while the opposite is true for the vertical case. Next, we can see that, as in the case of horizontal polarization, the resultant effect of moisture is greatest at 5 NMi for the vertical polarization case and there is little difference between the 30 NMi and 50 NMi cases. For this particular system, the absolute magnitudes of the peak powers of the two surfaces are greater for horizontal polarization than for the vertical polarization at all three separations. As far as the curves were plotted, the crossovers for vertical polarization are present for 5 NMi and 50 NMi while at horizontal polarization they occur for 30 NMi and 50 NMi. As is clear from this series of comparisons, moisture dependent effects are evident for both horizontal and vertical polarization and their respective roughness dependencies are dissimilar.

3.4 Wavelength

All the studies of this report so far have been for L-band frequencies. The next question to be addressed is the types of moisture effects that would be seen by the system operating at S-band with a signal wavelength of 0.1 m. As has been the procedure, we begin with Figure 15, where the effect of distance between antennas on the moisture dependence is shown. Then, the effect of moisture is shown as a function of surface roughness in Figure 16 and the results are compared with the corresponding sets of curves at $\lambda = 0.275$ m shown in Figure 5.

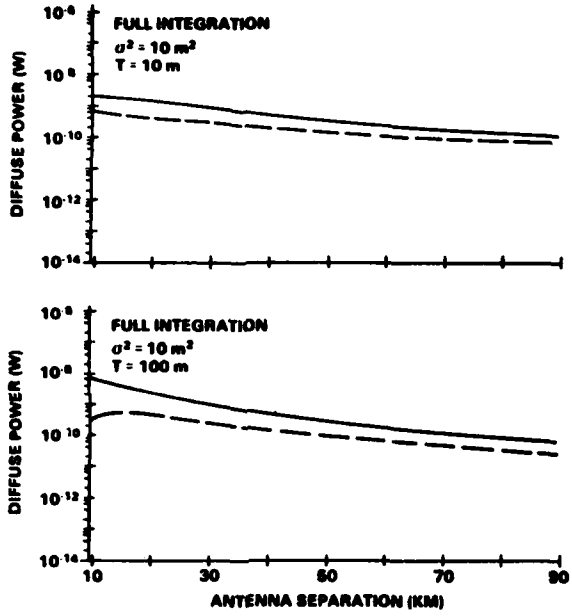

Figure 15. Diffuse Power vs Antenna Separation at a Wavelength, $\lambda = 0.1$ m, Full Integration Surface Model Without Shadowing, at Two Roughness Levels: —— $\epsilon = (2, 1.6)$, and — — — $\epsilon = (30, 0.6)$

3.4.1 INTRODUCTION

In Figure 15 we show results at two different roughness levels, $\sigma^2 = 10\ m^2$ and T = 10 m and 100 m. No shadowing is included. We can see that at this wavelength and short separations the diffuse power for the dry soil at T = 100 m is greater than that for T = 10 m while the reverse is true for the moist soil. There is little difference at large distances. Thus, at short separations the effect of moisture is greater

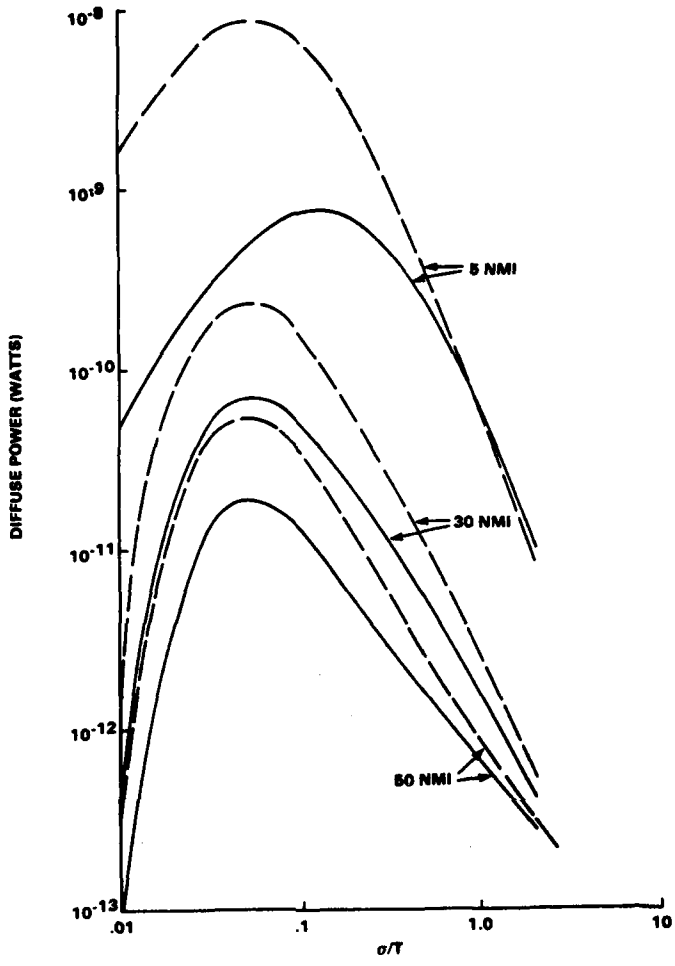

Figure 16. Diffuse Power vs Roughness at a Wavelength, λ = 0.1 m, Full Surface Model With Shadowing, at Three Antenna Separations: — — — ϵ = (2, 1.6), and —— ϵ = (30, 0.6)

for T = 100 m and relatively constant for most long separations. Comparing these results to corresponding ones with λ = 0.275 m, we see that for T = 100 m, there is more diffuse power for λ = 0.275 m but the relative effects of moisture appear to be about the same. For T = 10 m, there is more diffuse power at λ = 0.275 m and the overall effect of moisture appears slightly greater for that case.

3.4.2 ROUGHNESS EFFECTS

The roughness study of Figure 16 is for the usual system parameters except for wavelength. The full surface model is used and the effects of shadowing are included.

As has been true for all vertical polarization cases the diffuse power scattered from the dry surface at each distance is greater than that for the moist surface. The peak power decreases with separation and, except for the usual atypical 5 NMi moist surface case, the peaks occur at $\sigma/T \sim 0.05$. The effect of moisture is strongest at 5 NMi and is about the same for the 30 NMi and 50 NMi cases. There is a crossover at $\sigma/T \sim 1.0$ for the 5 NMi case and, although it does not occur within the range of the curves, it would seem that the 50 NMi case is tending towards a crossover. There is no clear sign of this at 30 NMi within the limits considered.

The comparisons with L-band results (Figure 5) show a number of similarities. The relative magnitudes of the moisture effects are equivalent. There is a factor of three difference between the displaced peak power levels at 30 NMi and 50 NMi and an order of magnitude at 5 NMi. The peaks (again, excepting the 5 NMi moist case) are at the same roughness and there are crossing points at 5 NMi and 50 NMi but not at 30 NMi. The absolute magnitudes of the power at the shorter wavelength are decreased by about an order of magnitude. The 50 NMi case at the longer wavelength shows a secondary peak at large roughness which is not in evidence at $\lambda = 0.1$ m. In general, though, the effect of moisture appears to be relatively insensitive to the differences in wavelength of the two frequency bands.

3.5 Antenna Configuration

The transmitting and receiving antennas of our baseline system are at different heights. This aspect controls the angles involved in the scattering of a given distance. Another related situation which we have already considered is the effect of azimuthal power pattern for the two antennas. In this section we will examine two additional positional considerations. The first aspect is the modification of the antenna heights such that either the two antennas are close to the surface or both are at a distance above the surface. This contrasts to the original mixed height configuration. Results are presented as a function of antenna separation. In the second instance, the antenna heights stay fixed but the heights of the transmitter and receiver are reversed. This is in distinction to the earlier case where just the azimuthal power patterns were switched. For this case the moisture effects are studied as a function of the surface roughness.

3.5.1 INTRODUCTION

In Figure 17 we employ the trajectory format to examine the effect of changing the relative heights of the two antennas. In our original cases we dealt with the situation where the transmitter was close to the surface while the receiving antenna was elevated to a considerable height above the ground. Here, either both antennas are near the surface or both are elevated. The two moisture levels are shown, the

signal is vertically polarized, the full surface model is used and the shadowing is not included. The two roughness conditions are depicted, $\sigma^2 = 10\ m^2$ and T = 10 m, 100 m.

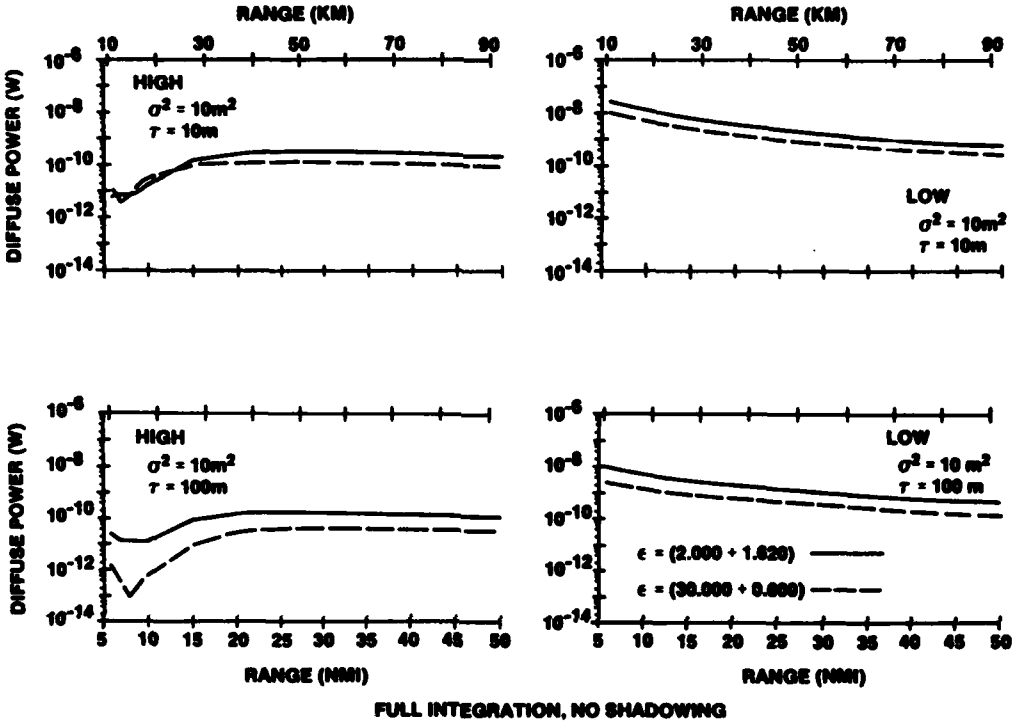

Figure 17. Diffuse Power vs Antenna Separation for Both Antennas High and Both Low, Full Surface Model Without Shadowing, at Two Roughness Levels: ____ $\epsilon = (2, 1.6)$ and_ _ _ $\epsilon = (30, 0.6)$

If we consider the raised antennas case we see that the effect of moisture is greater for the smoother surface but is still noticeable for the rougher surface. At distances greater than about 20 NMi the effect does not appear to be sensitive to separation. At short distances the behavior is distinctive. For T = 100 m the moist soil power levels show a more severe decline than the dry case. In the corresponding region for T = 10 m, the power levels for both soil conditions again decrease but in that instance the dry soil power is more affected. At some points it has even fallen below the power from the moist soil.

When the two antennas are both close to the surface, all curves of power are smooth, there is little change with separation at any distance. The effect of moisture is slightly greater for T = 100 m.

To see how these results fit into the picture we consider the corresponding cases when the antennas are not at the same height as shown in Figure 3. In those results the effect of moisture is stronger for T = 100 m as is true in Figure 17. However, the results are a mixture of trends from both high and low cases. The dual height power shows the decrease with distance that can be seen in the low height case but it is a stronger effect for the dual height case. In contrast, at short distances the dual height curves show the depressed levels of diffuse power of the elevated antenna case with the greater effect at T = 100 m. However, there is no sign of the crossover seen for T = 10 m. Similar diffuse power behavior as a function of antenna height have been shown in our earlier studies.[6]

The variety of effects seen as the respective positions of the two antennas are changed is not surprising since this also changes the range of angles in the integrations over the scattering surface, as well as the basic orientation of that surface. This simple analysis of the effects of distance above the surface can not hope to offer any definitive statement on the moisture effects that result, except to point out that there are differences in scattered power and that they do vary in extent from case to case. This question represents a study in its own right for any final conclusion.

3.5.2 ROUGHNESS EFFECTS

In Figure 18 we have the calculated diffuse scattered power for the two soil conditions as a function of roughness using the full integration model (including shadowing). As would be expected by the fact that the scattering and incident angles are altered by changing the respective antenna heights we see considerable variance in results as compared with the corresponding case of Figure 5 at the original antenna heights. The angles affect both the cross section of the surface elements and the reflection coefficients. A further difference is introduced by the fact that the power contributions are dependent on the angular variations in the two power patterns.

Before discussing the two cases we will first comment on the moisture effects as seen in Figure 18. For both soils the peaks in the three separation curves all occur at about $\sigma/T \sim 0.07$; no clearly variant behavior for 5 NMi is visible. For both soils, the 50 NMi case shows signs of the second peak (suppressed by shadowing) at high σ/T values and its plot crosses the power curves for both of the other separations. The difference due to moisture does not appear to be sensitive to separation and the peak power difference is about a factor of four or five in all instances. The three peak power levels are relatively close for the respective moisture contents and in fact, for the moist case, the 30 NMi peak actually exceeds that of the 5 NMi separation.

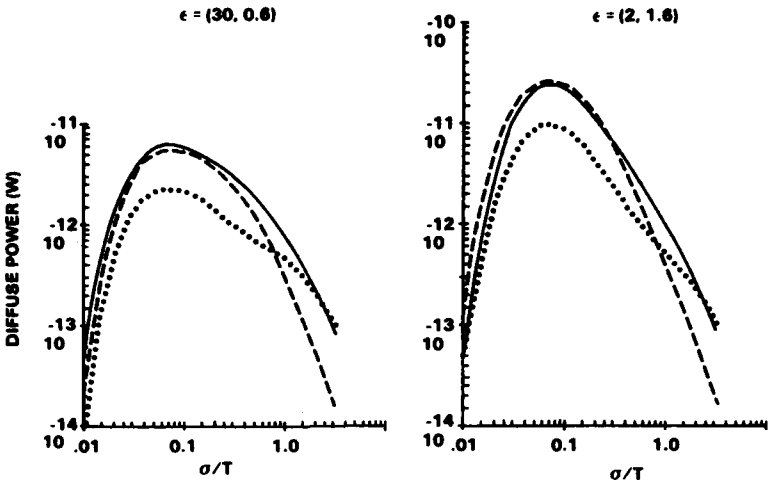

Figure 18. Diffuse Power vs Surface Roughness, Heights of Transmitter and Receive Antenna Reversed, Full Surface Model With Shadowing and ϵ = (2, 1.6), and ϵ = (30, 0.6): ——— 5 NMi, — — — 30 NMi, and .... 50 NMi

If we now compare these results with the original set of full integration results of Figure 5, we see that the reversal has reduced the original peak power levels. At 5 NMi the reversal results in a three order of magnitude decrease in peak power for both soil conditions. For 30 NMi and 50 NMi the reduction is about two and one-half orders of magnitude. The uniform peak location for the reversed case represents an increase in roughness compared to the original peaks at 30 NMi and 50 NMi and a decrease in roughness for 5 NMi. The reversed curves at 50 NMi showed the same secondary peak as the original. The crossover for the 30 NMi case for moist soil, which occurs prior to the peak values, is a unique result although the dry soil curves are quite close at those separations. In general, for this reversed case we can say that there is considerably less diffuse power, and the effect of moisture is decreased at 5 NMi and slightly increased at the larger distances. Finally, here, as in almost all the cases considered, the dependence of moisture effects on surface roughness shows some distinct and individual aspects.

4. DISCUSSION

The results in this report represent a broad spectrum of conditions and the effects of moisture can be quite distinct for some cases. We will summarize the results found in the various topic areas considered.

4.1 Scattering Model

The basic condition is that of vertical polarization and dual heights (transmitter close to surface), for the bistatic scattering system with an azimuthal monopulse receiving antenna power pattern at high altitude. The two models lead to a variety of results. In general, the dry soil power levels exceed those of the moist soil cases. The standard surface results show less moisture effect than is present when the general model is used. The results at 5 NMi seems anomalous, particularly for the standard case. For the standard surface, crossovers occur at large roughnesses for all separations while for the full integration there is no crossover for 30 NMi within the range of roughness considered. The full surface results at 50 NMi show a second peak at large roughness which is not evident in the standard model result. In both models the effects of shadowing are extremely important, particularly at large roughness levels. The standard model introduced some unusual slope variations to the curve of diffuse power vs roughness for the moist soil case and these appear for all separations at similar roughness parameters. Their relation to the violation of roughness contraints is uncertain. The overall variety in results serves to show that care must be taken in determining the effect of moisture, and that the use of the standard model which suppresses the effect can lead to discrepancies.

4.2 Moisture Level

An extremely general comment on moisture effects can be made. The difference in diffuse scattered power due to dielectric constant is minimal at both small roughless levels and large roughness levels, and is a maximum at some intermediate roughness levels.

Next, (as has been pointed out in the text) with some assumptions about the effect of ϵ_2, we can comment on the effect of successive increases in moisture level on the scattered power. In general, the peak power decreases with increasing moisture level but the magnitude depends on separation and ranges from a factor of three at 50 NMi to an order of magnitude at 5 NMi. The standard model results are similar at 30 NMi and 50 NMi but the behavior at 5 NMi is variant, particularly for the extremely moist cases. The slope variations in the standard model results can be seen to be moisture dependent in this series of results. As the moisture increases, they appear and are present for all separations at about the same roughness level. The relation of this result to roughness-constraint violations is uncertain.

4.3 Power Pattern

We begin the study of how antenna patterns affect the moisture-related results by replacing the original azimuthal power pattern of the receiver. Two cases are used. Both remove the monopulse condition. The patterns that replace it have a centerline peak power with two azimuthal tapers. The results indicate that this does not remove moisture effects but the presence of the peak tends to maintain the diffuse power at a relatively constant level as separation increases. The moisture effect is larger at 5 NMi than for the rest of the trajectory and, as the distance increases, the relative level of the effect remains fairly constant.

A second type of change was made wherein the azimuthal monopulse pattern was not replaced but was shifted to the transmitting antenna close to the surface while the transmitter's isotropic azimuthal pattern was assigned to the elevated receiving antenna. In this case the standard surface model is used. For these conditions we see that, as before, crossovers occur at larger roughness. The slope variations for the moist soil case appear to be enhanced by this pattern and the moist soil curves show a more gradual slope near their peaks when shadowing is not included. As a result, the effect of shadowing is to cause the moist surface results to peak at lower roughness levels. For this case the moisture effects tend to be suppressed, particularly at 30 NMi.

4.4 Polarization

The majority of the cases are for vertical polarization. Here we consider the results for horizontal polarization. In general, we find that the horizontally polarized signals result in greater amounts of diffuse scattered power than the vertically polarized signals. For the ranges considered, the moist soil results exceed those of the dry soil, which is in direct contrast to the situation in the vertical polarization cases. The effect is greatest at 5 NMi and, beyond that region, the relative effect remains essentially constant as separation increases. The effect of moisture is generally less than for vertical polarization. In addition, the roughness dependence is dissimilar. The full integration model does not appear to result in a crossover at 5 NMi and the roughness at which crossover occurs decreases with separation. This is a change from the corresponding crossover behavior at vertical polarization.

4.5 Wavelength

In this discussion we return to vertically polarized signals but change the wavelength of the signal to S-band (0.1 m). The results for moisture effects depend on separation and roughness. As was true for $\lambda = 0.275$ m the dry soil results exceed

the moist ones at $\lambda = 0.1$ m which is consistent with the polarization condition. Similarly, the results at 5 NMi are still anomalous and the effects of moisture are greatest near 5 NMi and remain relatively insensitive to distance at greater separations. The peak in the original results at 50 NMi does not appear in the $\lambda = 0.1$ m case. The overall assessment is that moisture effects are not particularly sensitive to wavelength for this system.

4.6 Bistatic Configuration

In this discussion we consider the effects that occur when both the antennas are elevated or both near the surface. For the former case the effect of moisture is greater for the smoother surface case but is still present as the roughness is increased. The effect is more pronounced at short separations and, at larger distances, is relatively constant. For the smooth surface at short distances, the drop in power for the moist case exceeds that for the dry; for the rougher surface the dry results decrease more sharply and even become less than the moist soil values near 5 NMi. When the two antennas are close to the surface the behavior of the curves with distance is regular and there is little effect of moisture with separation. The smoother surface cases show larger moisture effects for this set of antenna positions. The dual height results combine effects from the two equal height cases. The variability as a function of antenna height is not unexpected, in as much as this aspect affects the scattering angles and the orientation of the actual scattering surface.

A final topic, which is related to the previous one, addresses the case where the respective heights of the transmitter and receiver are reversed. As in the previous discussion, the angles and surface are affected and the switched positions result in a different behavior of moisture with roughness. This is a full integration result. The peak powers at the three separations all occur at the same roughness level. No distinctive 5 NMi behavior is seen but the indication of the second peak at large roughness for the 50 NMi case is present for both moisture levels. This results in the crossover of that curve with respect to the others. The three peak power levels for the respective moisture curves are quite close and, in fact, that of the 30 NMi case exceeds the peak of the 5 NMi case for the moist soil. This is the only example of pre-peak crossover in the range of cases considered. The effect of moisture is about the same at all separations, representing an increase in effect for the 30 NMi and 50 NMi conditions of the original configuration and a corresponding decrease in effect at 5 NMi.

5. CONCLUSIONS

The range of topics considered in this report is extensive and thus there are a corresponding number of findings that are related to individual aspects of the analysis. These have been examined in the detailed discussions of the specific factors in Section 4. Here we are limiting ourselves to some general comments.

In this assessment it should be stressed that we have tried to go beyond simple statements about properties at a single scattering angle and have shown actual integrated effects corresponding to various bistatic scattering configurations. The resultant moisture related effects are quite varied. For vertical polarization, the dry soil results exceed the moist while the reverse is true for the horizontal polarization case. Reversing the height of transmitter and receiver resulted in massive changes in power. The roughness dependence of moisture effects also varied from case to case. The most significant moisture effects are at short antenna separations and beyond that region the effect is relatively independent of distance. The use of the conventional glistening surface showed a tendency to de-emphasize the relative effect of moisture. As a general rule, the use of the conventional model requires careful consideration in as much as there are the inherent roughness limitations contained in its formalism. In addition, even for small roughness, the parallelisms in the geometry are suspect at short antenna separations. The alternative model, which uses the radar footprint and azimuthal variations in surface cross section, does not depend on those model constraints and hence is quite general. The final point is that some moisture effects could almost always be found and the combination of positional, roughness, and moisture content effects makes it extremely difficult to predict a priori the maximum diffuse scattered power for a surface.

References

1. Papa, R. J., Lennon, J. F., and Taylor, R. L. (1980) Prediction of Electromagnetic Scattering for Rough Terrain Using Statistical Parameters Derived From Digitized Topographic Maps, RADC-TR-80-289, AD A094104.
2. Papa, R. J., and Lennon, J. F. (1980) Electromagnetic Scattering From Rough Surfaces Based on Statistical Characterization of the Terrain, presented at International Radio Science Symposium (URSI), Quebec, Canada
3. Papa, R. J., Lennon, J. F., and Taylor, R. L. (1980) Electromagnetic Wave Scattering From Rough Terrain, RADC-TR-80-300, AD A09839.
4. Papa, R. J., Lennon, J. F., and Taylor, R. L. (1981) An Improved Model for Scattering From Rough Terrain, presented at the International Radio Science Symposium (URSI), Los Angeles, California.
5. Beckmann, P., and Spizzichino, A. (1963) The Scattering of Electromagnetic Waves From Rough Surfaces, MacMillan Company, New York.
6. Papa, R. J., Lennon, J. F., and Taylor, R. L. (1982) The Need for an Expanded Definition of Glistening Surface, RADC-TR-82-271, AD A130431.
7. Papa, R. J., Lennon, J. F., and Taylor, R. L. (1982) Further Considerations in Models of Rough Surface Scattering, RADC-TR-82-326, AD A130424.
8. Ruck, G. T., Barrick, D. E., Stuart, W. D., and Krichbaum, C. K. (1970) Radar Cross Section Handbook, Vol. 2, Plenum Press, New York.
9. Papa, R. J., Lennon, J. F., and Taylor, R. L. (1984) The Use of the Glistening Surface Concept in Rough Surface Scattering, RADC-TR-84-159.
10. Long, N. W. (1975) Radar Reflectivity of Land and Sea, Lexington Books.
11. Kerr, D. E. (1951) Propagation of Short Radio Waves, McGraw-Hill, New York.
12. David, P., and Voge, J. (1969) Propagation of Waves, Pergamon Press, Oxford.
13. Meeks, M. L. (1982) Radar Propagation at Low Altitudes, Artech House, Dedham.
14. Njoku, E. G., and Kong, J. A. (1977) Theory for passive microwave remote sensing of near surface soil moisture, J. Geophys. Res. 82:3108-3118.

Appendix A

The General Scattering Model

In this simplified analysis the starting point is the integral describing the diffuse scattered power. Its form is

$$P_{DIFF} = \left(\frac{P_T X_{LOSS} \lambda^2}{(4\pi)^3}\right) \iint \left(\frac{G_{TR}^{AZ}(\phi_2)\, G_R^{AZ}(\phi_1)}{R_1^2\, R_2^2}\right) \cdot \left(G_{TR}^{EL}(\theta_1)\, G_R^{EL}(\theta_2)\, \sigma^\circ(\theta_1, \theta_2, \phi_1)\right) \cdot dS$$

where

X_{LOSS} = system processing losses,

P_T = transmitted power,

λ = wavelength,

G_{TR}^{AZ} = gain (power) of transmitter in azimuth,

G_R^{AZ} = gain of receiver in azimuth,

G_{TR}^{EL} = gain of transmitter in elevation,

G_R^{EL} = gain of receiver in elevation,

θ_1 = elevation angle between boresight and point on glistening surface for transmitter,

θ_2 = elevation angle between boresight and point on glistening surface for receiver,

R_1 = range between transmitter and point on glistening surface,

R_2 = range between receiver and point on glistening surface,

dS = element of area of glistening surface which is illuminated by beacon,

ϕ_1 = azimuthal angle between boresight and point on glistening surface for receiver,

ϕ_2 = azimuthal angle between boresight and point on glistening surface for transmitter.

The diffuse power integral contains an expression for the normalized average bistatic rough surface cross section, σ°, which comes from Ruck et al.[8] The expressions derived by Ruck are quite general and highly complicated. The different forms of σ° used in the models will be discussed. We first give the general integration case and then indicate how the usual simplifications that include the Beckmann and Spizzichino surface model are developed. The normalized rough surface scattering cross section is given by

$$\sigma^\circ = |\beta_{pq}|^2 \, J \, S$$

where β_{pq} represents the scattering matrix contributions, S is the local shadowing function,[3] and the term J is related to the surface height distributions and the surface slopes. The shadowing function clearly depends on the roughness of the surface, and introducing this factor into the analysis can have significant effects on the diffuse scattered power (see Papa et al[6]). For our case of exponentially distributed heights, the general asymptotic form for J is

$$J = \left(\frac{3T^2}{\sigma^2 \xi_2^2}\right) \exp\left[-\left(\frac{\sqrt{6}T}{2\sigma}\right)\left(\frac{\xi_x^2 + \xi_y^2}{\xi_z^2}\right)^{1/2}\right]$$

where

$\xi_x = \sin\theta_i - \sin\theta_s \cos\phi_s$,

$\xi_y = \sin\phi_s \sin\theta_s$,

$\xi_z = -\cos\theta_i - \cos\theta_s$,

ϕ_s = azimuthal scattering angle,

θ_i = angle of incidence (with respect to surface normal),

and

θ_s = angle of scattering (with respect to surface normal).

It is in the scattering matrix term that the dielectric constant representing the respective moisture content levels is introduced. In that term, the matrix elements for linear polarization states are

$$\beta_{VV} = \left(\frac{a_2 a_3 R_{\parallel}(\theta_i') + \sin\theta_i \sin\theta_s \sin^2\phi_s R_{\perp}(\theta_i')}{a_1 a_4} \right)$$

$$\beta_{HV} = \sin\phi_s \left(\frac{-\sin\theta_i a_3 R_{\parallel}(\theta_i') + \sin\theta_s a_2 R_{\perp}(\theta_i')}{a_1 a_4} \right)$$

$$\beta_{VH} = \sin\phi_s \left(\frac{\sin\theta_s a_2 R_{\parallel}(\theta_i') - \sin\theta_i a_3 R_{\perp}(\theta_i')}{a_1 a_4} \right)$$

$$\beta_{HH} = \left(\frac{-\sin\theta_i \sin\theta_s \sin^2\phi_s R_{\parallel}(\theta_i') - a_2 a_3 R_{\perp}(\theta_i')}{a_1 a_4} \right)$$

Here, $R_{\parallel}(\theta_i')$ and $R_{\perp}(\theta_i')$ are Fresnel reflection coefficients

$$R_{\parallel}(\theta_i') = \frac{\epsilon_r \cos\theta_i' - \sqrt{\epsilon_r - \sin^2\theta_i'}}{\epsilon_r \cos\theta_i' + \sqrt{\epsilon_r - \sin^2\theta_i'}}$$

and

$$R_{\perp}(\theta_i') = \frac{\cos\theta_i' - \sqrt{\epsilon_r - \sin^2\theta_i'}}{\cos\theta_i' + \sqrt{\epsilon_r - \sin^2\theta_i'}} .$$

Note that ϵ_r is the relative complex dielectric constant of the surface, the subscript $\parallel$ refers to the E-field in the plane of incidence, and the subscript $\perp$ refers to the E-field normal to the plane of incidence. The remaining angle-related terms are

$$\cos \theta_i' = \frac{1}{\sqrt{2}} \sqrt{1 - \sin \theta_i \sin \theta_s \cos \phi_s + \cos \theta_i \cos \theta_s}$$

$$a_1 = 1 + \sin \theta_i \sin \theta_s \cos \phi_s - \cos \theta_i \cos \theta_s$$

$$a_2 = \cos \theta_i \sin \theta_s + \sin \theta_i \cos \theta_s \cos \phi_s$$

$$a_3 = \sin \theta_i \cos \theta_s + \cos \theta_i \sin \theta_s \cos \phi_s$$

and

$$a_4 = \cos \theta_i + \cos \theta_s .$$

In the general case, the diffuse scattered power is determined by integrating the product of the expression for σ° and the corresponding elevation and azimuthal receiver and transmitter gain factors over the region between the two antennas. The azimuthal integration is bounded by the extent of the azimuthal difference pattern (for a discussion of the technique used to introduce these bounds into formulation, see Papa, Lennon and Taylor[3]). In the results, this is referred to as the full scattering surface model.

Appendix B

The Simplified Standard Model

In the alternative scattering model the assumption is made that the receiver is sufficiently far from the transmitter that the portion of the "glistening surface" that contributes to the diffuse multipath is a long, narrow strip extending between the transmitter and receiver. This assumption allows us to make the approximation that the azimuthal scattering angle $\phi_s \approx 0°$ and results in a considerable simplification (and difference) in the $\sigma°$ calculation.

In the scattering matrix, the first consideration is that the two cross-polarized terms are now zero. Only the co-polarized elements contribute to the scattering. In those cases, manipulation of the relations and introducing the angle α

$$\alpha = \left(\frac{\theta_i + \theta_s}{2} \right)$$

leads to

$$\beta_{VV} = \frac{(1 + \cos 2\alpha)\, R_{\parallel} (\theta_i)}{(\cos \theta_i + \cos \theta_s)} \qquad \text{(vertical polarization)}$$

and

$$\beta_{HH} = \frac{(1 + \cos 2\alpha)\, R_{\perp} (\theta_i)}{(\cos \theta_i + \cos \theta_s)} \qquad \text{(horizontal polarization)} .$$

In these two terms it should be noted that each depends on only one Fresnel reflection component while in the general solution each includes contributions from the two Fresnel coefficients. Another effect of this assumption is seen in the terms ξ_x, ξ_y, and ξ_z. These reduce to

$$\xi_x = \sin\theta_i - \sin\theta_s$$

$$\xi_y = 0,$$

$$\xi_z = -\cos\theta_i - \cos\theta_s .$$

As a result we then have

$$J = \left(\frac{3T^2}{\sigma^2 \xi_z^2}\right) \exp\left[-\left(\frac{\sqrt{6}\,T}{2\sigma}\right)\left(\frac{\xi_x^2}{\xi_z^2}\right)^{1/2}\right] .$$

Since this has effectively removed any azimuthal variation in $\sigma°$, the calculation of the diffuse power scattered by the surface and received at the antenna is approached differently. In this model, the surface of integration is determined by the Beckmann and Spizzichino definitions of glistening surface length and width. The length is obtained by calculating the location of the two end points of the glistening surface. For a homogeneous surface, the distance from the two end points to the transmitter and receiver (L_1, L_2) are based on the respective heights (H_A, H_T) and a roughness factor (σ/T) where σ^2 is the surface height variance and T is the correlation length. Then

$$L_1 = H_A \cot(2\beta_o)$$

and

$$L_2 = H_T \cot(2\beta_o)$$

where

$$\tan\beta_o = 2\sigma/T .$$

It should be noted at this point that, although the length and width calculations start from the same initial premise, their derivations are separate. This is pointed out to clarify some limitations implicit in the use of this model and to emphasize the two approaches to the calculation of length and width in this study.

The starting point is that the glistening surface of interest is that extent of surface from which the diffuse scattered power is equal to or greater than 1/e of its maximum. By using the asymptotic expression for σ° valid for large surface roughness, we can show that, for that condition to be satisfied $\measuredangle\beta \leqq \measuredangle\beta_o$ over the surface. Here $\measuredangle\beta$ is the angle between the vertical axis and the bisector of the angle between the line connecting the transmitter to a point on the surface and the line from that point to the receiver. The boundary of the surface is the locus of points for which $\measuredangle\beta = \measuredangle\beta_o$. We first consider these concepts in relation to L_1 and L_2. Their defining relations require the assumption that the line to the surface point from the transmitter or receiver, respectively, forms the angle $2\beta_o$ with the horizontal axis. This can be derived from the above concepts and additional assumptions of parallelism. Thus, for the length conditions, $\measuredangle 2\beta_o < 90^\circ$ and $\sigma/T \leqq 0.5$. At that roughness $L_1 = L_2 = 0$, and the surface extends across the entire separation between the two antennas. In this report we replace the original L_1 and L_2 length calculation by the entire separation distance for $\sigma/T \geqq 0.5$.

Next, we consider the concepts that pertain to the width of the surface. The form used here, as derived by Beckmann and Spizzichino, includes the assumption that $H_A \ll X_1$, $H_T \ll X_2$, and $W \ll X_1$, X_2 where W is the local surface width. As roughness increases, L_1, $L_2 \rightarrow 0$, and the height constraints are violated. Eventually, the width to axial distance ratio also becomes inconsistent.

A more complete discussion of glistening surface definitions and constraints is presented in Papa et al.[9] The point from that report that is significant here is that, despite the violation of the constraints on the Beckmann and Spizzichino model, the resultant power calculations for large roughness conditions give values that are not unreasonable. Indeed, the most serious problems appear to occur for small roughness levels. Thus, the moisture effects calculated by this model are presented at roughness levels for which the original assumptions and constraints are not strictly satisfied. In line with the patterns of the results and the discussions in the more comprehensive surface study,[9] the indicated moisture trends are not unreasonable for most cases. It should be noted that these restrictions are not contained in the more general model of this report with which these standards results are compared.

We have discussed the surface length and width concepts and shown how the length is determined. The next consideration is to show the corresponding formula for the width as given by this model. Beckmann and Spizzichino calculated that along the extent of the surface, the local width W is given by

$$W = \left(\frac{2X_1X_2}{D}\right)\left(\frac{H_A}{X_1} + \frac{H_T}{X_2}\right)\left[\tan^2\beta_o - 0.25\left(\frac{H_A}{X_1} - \frac{H_T}{X_2}\right)^2\right]^{1/2}.$$

Here,

D = total ground distance from transmitter to receiver,

X_1 = distance from transmitter to point on glistening surface,

and

X_2 = distance from receiver to point on glistening surface.

In the actual calculation, $\tan\beta_o$ is not limited in the width determination but is allowed to take on any value that results from the surface roughness, where we vary σ/T in this study so that $0.1 \leqq \sigma/T \leqq 3.0$.

Once these quantities have been determined, the diffuse scattered power contribution from each increment of length along the glistening surface is obtained by multiplying the product of the centerline value of $\sigma°$ and W by the appropriate azimuthal and elevation plane antenna power pattern distributions.

Appendix C

Detailed Comparison for the Two Models

In the discussions of the text we have introduced the effect of surface moisture content on scattering for several system parameters as determined by the physical optics model. In Appendix B we discussed the implications of using a simplified scattering model including the Beckmann and Spizzichino definition of the scattering surface dimensions. In this appendix we will present detailed comparisons of the results obtained by the two versions of the scattering model. Comments will be made on the effect for the different scattering system parameters.

The first topic is the detailed consideration of the differences in the roughness dependence of the moisture effects for the two models. The three antenna separations are considered separately.

Figure C1 depicts, for the full integration surface model at 5 NMi separation, the variation in diffuse scattered power as a function of σ/T; the curves extend over several orders of magnitude in roughness factor. The basic results, which do not take shadowing into account, are represented by the dashed lines. Several comments can be made. For both moisture values the variation with roughness is similar. The sandy soil curve peaks at a higher value (6.5×10^{-8} W) than that for the moist soil (7.5×10^{-9} W). The peak for the moist case occurs at a larger slope value (σ/T) that is, $\sigma/T \sim 0.17$ vs $\sigma/T \sim 0.06$. It should also be noted that without shadowing the sandy results remain greater than the moist values over the range of slopes considered although for large slope values the two curves are approaching each other. When shadowing is introduced into the analysis (solid

curves), several aspects are affected. The most obvious difference is that for both moisture cases the effect on the diffuse power is greater for the larger slope regimes. Secondly the peak for the moist case now occurs closer to the peak for the sandy soil case. The reason for this is that the integrated shadowing contributions for the moist soil in this instance begin to be effective at a slightly smoother condition than that at which the peak occurs. In fact, the moist soil peak diffuse power as a function of σ/T is now somewhat less, while the peak for the sandy soil remains unchanged. Another change from the unshadowed result is that the curve of shadowed diffuse power for the sandy soil undergoes a crossover with the moist shadowed power curve near $\sigma/T = 1$.

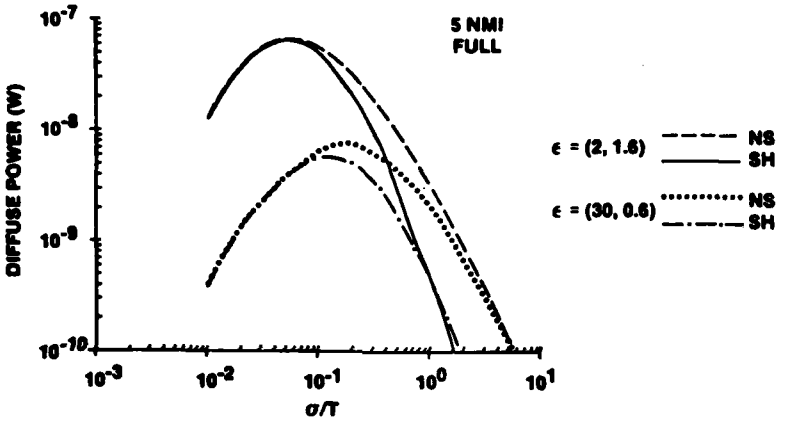

Figure C1. Diffuse Power vs Roughness, Full Surface Model, $\epsilon = (2, 1.6)$ and $\epsilon = (30, 0.6)$, at a Separation of 5 NMi, With Shadowing and Without Shadowing

Figure C2 addresses the same set of conditions when the standard approximation for the glistening surface boundaries is employed in the calculations. The dashed curves (unshadowed) show that the sandy soil diffuse power has a dependence on σ/T considerably different from that for the moist surface. Although the peak values ($\sim 2 \times 10^{-9}$W) are comparable, the sandy peak extends over almost an order of magnitude in σ/T while the moist soil peak is fairly sharp and occurs at a considerably larger σ/T ratio (~ 3). For this glistening surface case, the sandy unshadowed results do not remain greater than the corresponding moist values for all σ/T but cross over at $\sigma/T \sim 1.5$. The oscillatory slope pattern that is visible in the curves for the moist soil has been confirmed by an extensive study of cases in the σ/T range of interest, but there is no such trend for the sandy soil condition.

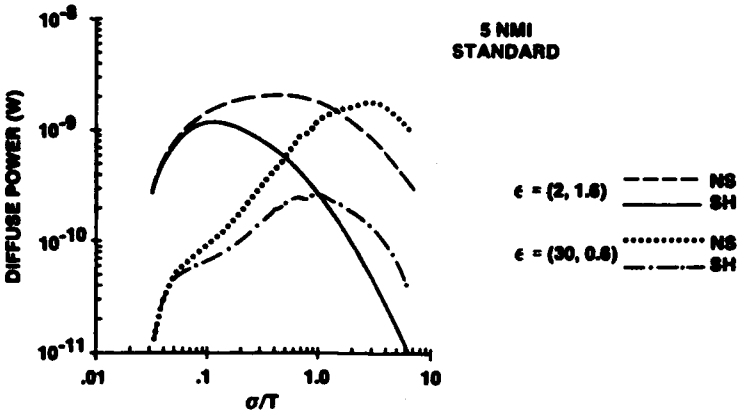

Figure C2. Diffuse Power vs Roughness, Standard Surface Model, ϵ = (2, 1.6) and ϵ = (30, 0.6), at a Separation of 5 NMi, With Shadowing and Without Shadowing

This will be discussed further. The shadowing results are interesting. Again, the moist soil shadowing results appear at a slightly smaller σ/T ratio than the dry soil case. In this figure, both sets of curves show reduced peaks and the increasing importance of shadowing at large σ/T narrows the extent of the dry soil peak power. The peak shadowed power for the moist case occurs at a lower σ/T value ($\sim$ 1.0) than is the case for the unshadowed results. The crossover pattern for the two cases is present for the shadowed case also, but it occurs at that value of σ/T = 1.0. Above σ/T = 1.5, the effect of shadowing reduces both soil diffuse powers by an order of magnitude.

For an antenna separation of 30 NMi the full surface results are shown in Figure C3. For both shadowed and unshadowed conditions, the sandy soil results are greater than the moist ones. Both unshadowed peaks (3.8×10^{-9} W; 1.2×10^{-9} W) occur close together on the roughness scale as do the shadowed peaks. The shadowing reduces the peak power for both types of soil by a factor of two, but at small slope values it is not clear that the effect is more prominent for one case than the other. At this antenna separation, neither set of curves shows a crossover in magnitude at large σ/T. Above $\sigma/T \sim 0.5$ the shadowed power is more than an order of magnitude less than the unshadowed for both soil types.

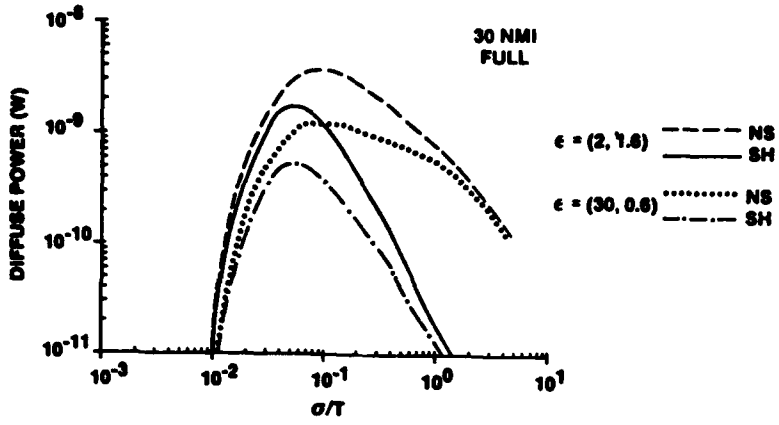

Figure C3. Diffuse Power vs Roughness, Full Surface Model, ϵ = (c, 1.6) and ϵ = (30, 0.6), at a Separation of 5 NMi; With Shadowing and Without Shadowing

In Figure C4 the results obtained are those for a separation of 30 NMi under the usual glistening surface assumptions. The unshadowed sandy soil results peak (4×10^{-11} W) at about $\sigma/T = 0.5$ roughness while the moist soil case shows no peak in diffuse power. The slope changes are present in the moist soil results for $0.4 \leq \sigma/T \leq 1.0$ and the crossover in power occurs $\sigma/T \sim 3.5$. When shadowing is introduced, the peak sandy soil power is reduced by a factor of five. Within the range of roughness considered, it is not clear that any significant difference in effect occurs for small σ/T. It is interesting to note that for the shadowed moist surface, a peak does occur at about the same roughness level (0.025) as the sandy case. The slope oscillations are present for the moist case, the effects are more pronounced at large roughness, and the crossover occurs for $\sigma/T \sim 2.4$. Above $\sigma/T \sim 0.35$, shadowing reduces the power for both soil types by at least an order of magnitude.

Figure C5 shows the complete surface results for a separation of 50 NMi. The peak unshadowed values (1.5×10^{-9} W; 4.6×10^{-10} W) occur close to one another at $\sigma/T \sim 0.1$. In this case a single large scale secondary maximum is present for both soil cases at large σ/T. The crossover appears at $\sigma/T \sim 4.0$. Shadowing reduces the peak powers by a factor of three and shifts them to a smaller σ/T ratio (~ 0.05) but maintains their coincident occurrence. No difference in onset is noticeable and the crossover appears at $\sigma/T \sim 3.0$. The large scale effects of shadowing for $\sigma/T > 1.0$ have tended to suppress the secondary maxima, particularly for the moist soil. At these values the shadowing effect has increased to the point that the reduction in power is as much as two orders of magnitude.

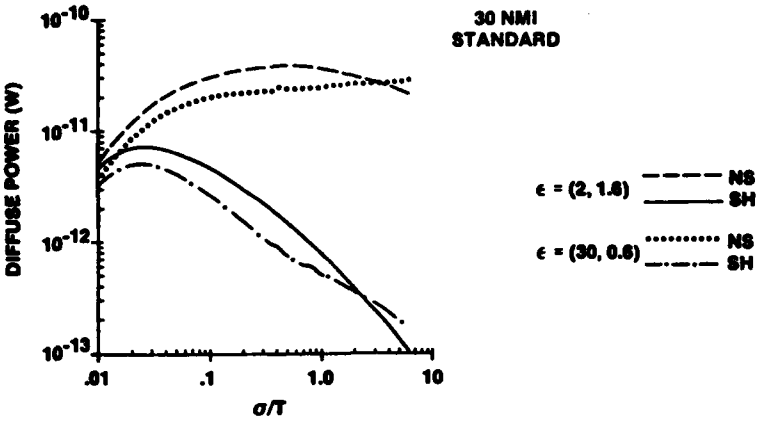

Figure C4. Diffuse Power vs Roughness, Standard Surface Model, ϵ = (2, 1.6) and ϵ = (30, 0.6) at a Separation of 30 NMi; With Shadowing and Without Shadowing

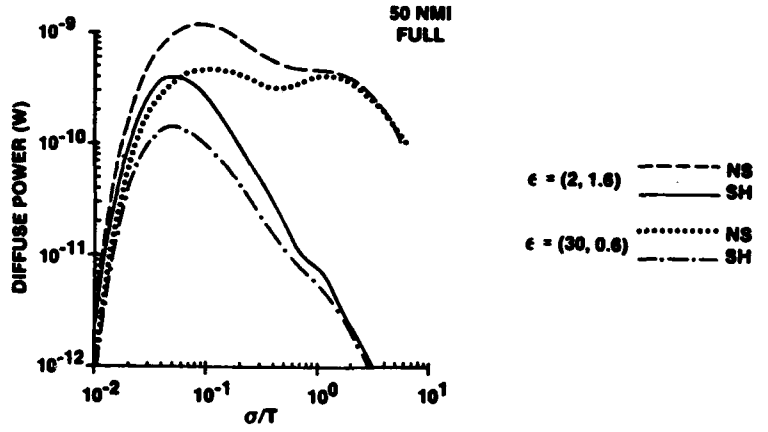

Figure C5. Diffuse Power vs Roughness, Full Surface Model, ϵ = 2, 1.6), and ϵ = (30, 0.6), at a Separation of 50 NMi; With Shadowing and Without Shadowing

The 50 NMi results for the standard assumptions are shown in Figure C6. Both unshadowed curves are similar up to $\sigma/T \sim 0.4$ where the dry soil power peaks (1×10^{-11} W) and then begins to drop while the moist soil results continue on a plateau ($\sim 6.7 \times 10^{-12}$ W). The sandy values cross those for the moist soil at $\sigma/T \sim 3.2$. Again, slope variations are present for the moist soil case but not for the dry surface. At the smallest roughness values considered, both shadowing

effects are well established. The peaks (1.2×10^{-12} W; 9.5×10^{-13} W) occur at $\sigma/T \sim 0.016$ and are an order of magnitude less than the levels reached without shadowing. The crossover is present at $\sigma/T \sim 2.3$ and the moist soil slope variations occur for $0.4 \leqq \sigma/T \leqq 1.0$. The shadowing-induced reduction in power exceeds an order of magnitude for both curves beyond $\sigma/T \sim 0.07$.

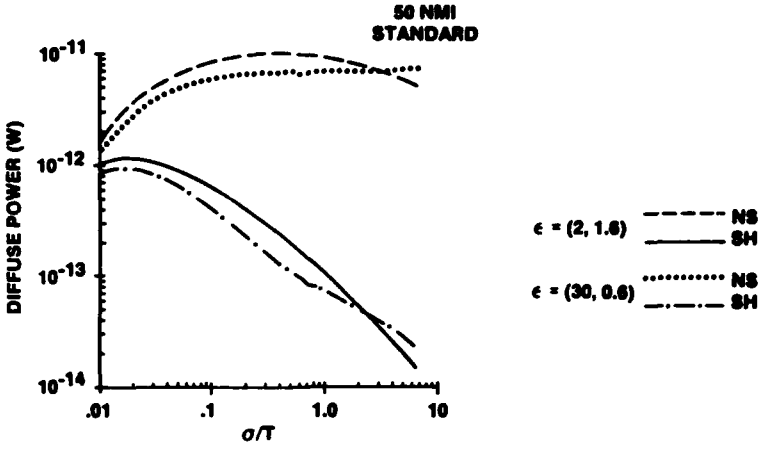

Figure C6. Diffuse Power vs Roughness, Standard Surface Model, $\epsilon = (2, 1.6)$ and $\epsilon = (30, 0.6)$ at a Separation of 50 NMi; With Shadowing and Without Shadowing

Now that the individual figures have been examined, we can compare different combinations to look for trends. Examination of the full surface results (Figure C1, Figure C3, and Figure C5) shows that the effect of the shadowing for both moisture levels at 30 NMi and 50 NMi is to cause the peaks to occur at a lower σ/T value, which is equivalent to the peak location for the dry soil case at 5 NMi where there is no shadowing induced change. The only discrepancy is the moist soil peak at 5 NMi and, even in that instance, the shadowing does introduce a slight move in the peak towards the lower roughness position. For the cases that include shadowing, the crossover pattern is unusual in that it is present at 5 NMi at $\sigma/T < 1$, is not evident at 30 NMi (even for $\sigma/T \sim 6$) and returns at 50 NMi but at $\sigma/T \sim 3$. At both separations where crossover occurs the shadowed case occurs at smaller σ/T than does the unshadowed. At the larger σ/T values the effect of shadowing becomes more pronounced as the separation is increased.

The comparisons are not so simple for the corresponding cases (Figure C2, Figure C4, and Figure C6) under the assumption of the standard Beckmann and Spizzichino bounds for the glistening surface. At 5 NMi, where the unshadowed

surface results have peak locations that differ by an order of magnitude in roughness, there is some decrease in roughness for the shadowed peak locations, but they still occur an order of magnitude apart. In contrast, the 30 NMi and 50 NMi unshadowed results have only a plateau for the moist soil. For shadowing, though, both surfaces have peaks and they occur at about the same roughness at both separations ($\sigma/T \sim 0.02$). Note that this is below the value where the scattering surface vanishes at 5 NMi. There are slope variations in the moist soil curves for both shadowed and non-shadowed results at all separations. For both soils, the cross-over is present at all three separations for both shadowing and no shadowing. In all instances, the shadowed crossover occurs at smaller σ/T values than the unshadowed one. The σ/T ratio at which shadowing reduces the power for both soil types by at least an order of magnitude decreases as the separation increases.

The comparisons make it clear that the effect of shadowing is significant for a wide range of conditions and hence should be included for accurate prediction of the diffuse scattered power.

In Section 3.1.3 we discussed the effect of moisture for successively increasing levels of moisture. Here we introduce the equivalent cases, as calculated by the standard model. The additional results for the standard model are shown in Figure C7. These have to be related to the standard case results of Figure 5 to see the progression of results. This figure also allows us to examine the slope changes seen for the moist cases at additional conditions.

The discussion of this set of results is interesting. If we consider the full integration cases we see that the general pattern is similar for the entire range of conditions. The peak power decreases with increasing moisture. However, the effect depends on the separation and varies from a factor of three difference at 50 NMi to an order of magnitude at 5 NMi. Moreover the peak is shifting to slightly larger roughness values for the extremely moist cases at 5 NMi while there does not appear to be an equivalent shift at lower moisture levels.

For the standard cases the curves for 30 NMi and 50 NMi are extremely close for all moistures. At the 5 NMi separation the general trends are similar except for the extremely moist case. All three other cases show a shifted peak ($\sigma/T \sim 0.1$) with a change of about a factor of two in peak power which is again different from the other separations. The curve for the extremely moist case is considerably variant from those of the other cases. It peaks at an order of magnitude greater roughness than the others and has a distorted slope. Its peak drops sharply (a factor of four less than that of the dry case) and no similarity to the remaining cases is evident.

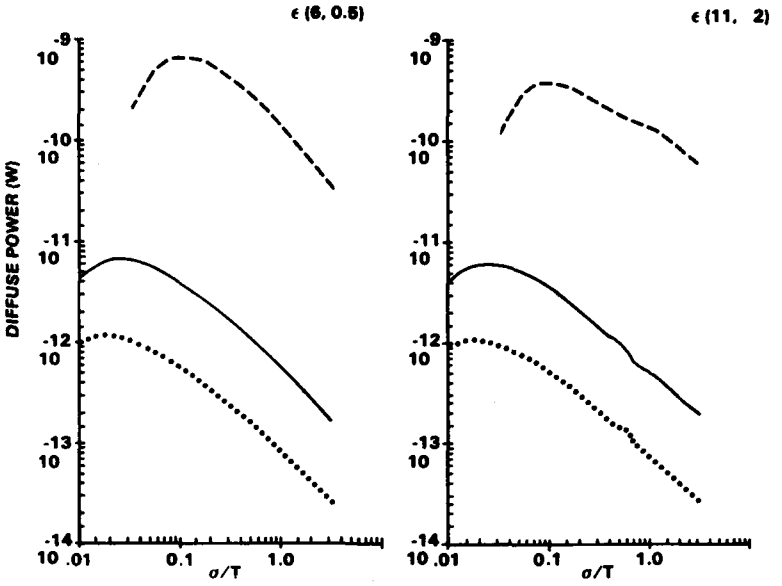

Figure C7. Diffuse Power vs Roughness, Standard Surface Model With Shadowing, ϵ = (6, 0.5), and ϵ = (11, 2): ---- 5 NMi, ____ 30 NMi, and ..... 50 NMi

This series of curves confirms that the slope variations are moisture related. There are no indications of slope variations for the relatively dry cases but as the moisture increases the variations appear. They are present at all separations when they appear, even for the anomalous 5 NMi extremely moist case. When present, their constant roughness relationship is independent of moisture or separation, again including the anomalous case. Also, the full integration results show no sign of this behavior for any separation or for any degree of moisture in the soil.

The comparison of the full integration results with those of the standard solution shows that the standard approach for these system parameters would show no effect of moisture at 30 NMi or 50 NMi while the more exact solution changes by a factor of three or four; at 5 NMi the standard solution shows changes of a factor of two (four in the extreme case) whereas the full integration solution changes more than an order of magnitude.

It should be stressed that the magnitudes shown here are for the particular set of system conditions used, but the differences suggest that careful consideration should be given when using standard solution methods to evaluate the effect of moisture on rough surface scattering of electromagnetic waves. The next section of this report examines how changes in various conditions affect the diffuse power.

Following the sequence of results analyzed in the text we next address the detailed analysis of the cases at each separation for the antenna with reversed azimuthal power patterns. These results are shown in Figure 12 for the simplified model.

If we examine the diffuse power at 5 NMi, we see that the anomalous moist surface behavior is present with the unshadowed peak (2.3×10^{-9} W) occurring at $\sigma/T \sim 1.0$ whereas the dry soil peak (1.2×10^{-8} W) occurs at $\sigma/T \sim 0.1$. Both soils show the crossover effect in the shadowed and unshadowed cases. The reduction in peak power for shadowing is greater in the moist soil case since the peak occurs at a point where shadowing effects are stronger due to the increased roughness. Thus the effects of shadowing is to bring the peak location for the moist case closer to that of the dry soil peak. For $\sigma/T \geq 2$ shadowing reduces both sets of results by about an order of magnitude. The unusual slope changes in the moist soil case are present in both curves.

At 30 NMi the more typical patterns are again present. The unshadowed dry and moist soil results peak relatively close together (4×10^{-10} W; 1.5×10^{-10} W) with the moist soil case having a more gradual slope near the peak. As a result of this, when shadowing is included in the calculation, the peak for the moist case occurs at a smoother surface condition than that of the dry soil. The effect of shadowing reduces the peak power by a factor of three or four. Crossovers occur in both sets of curves and above $\sigma/T \sim 0.35$, shadowing reduces the power for both soil types by at least an order of magnitude. The secondary peaks in the moist surface case are present as expected.

At 50 NMi we see that again both unshadowed peaks (1.5×10^{-10} W; 5×10^{-11} W) are similarly located. The sandy values cross those for the moist soil at $\sigma/T \sim 2.0$. At the smallest roughness values considered, shadowing effects are well established. The peaks (2×10^{-11} W; 1×10^{-11} W) are a factor of five less than the unshadowed ones, occur at lower σ/T values, and are not at the same point (the moist peak precedes the dry which is again consistent with the more gradual slope near the maximum for the moist case). Shadowing reduces power by an order of magnitude for both cases above $\sigma/T \sim 0.2$ and crossovers are present for both shadowed and unshadowed results. Secondary maxima are present for the moist soil case but not for the dry surface.

If we compare the present results with the corresponding ones in Figure C2, Figure C4, and Figure C6, we see that the general effect of changing the antenna pattern is to increase the peak power by an order of magnitude in all instances. At all separations, the steeper slopes near the peak of the dry soil case for the new pattern, are much more similar to the slopes of the moist soil cases in the original antenna pattern results than are the gradual moist surface slopes of this new pattern.

For both patterns, the 5 NMi results are atypical. Also, at 30 NMi and 50 NMi the moist soil unshadowed cases tended not to peak but maintained a slight rise. Another distinction is that the modified pattern tended to enhance the magnitude of the secondary slope variations for the moist soil case.

The study of how the use of the simplified model affects the results continues with the case where the polarization of the signal has been changed to horizontal polarization.

To examine how the different scattering surface model affects the results we present the standard model results in Figure C8. At all three roughness levels there is virtually no effect of moisture (the moist soil results are negligibly higher at close distances). The power trends are typical of the standard surface model with the overprediction at large separations and vanishing surfaces for the smooth surface conditions. Thus, use of the standard models leads not only to incorrect power levels but also to suppression of the moisture effects.

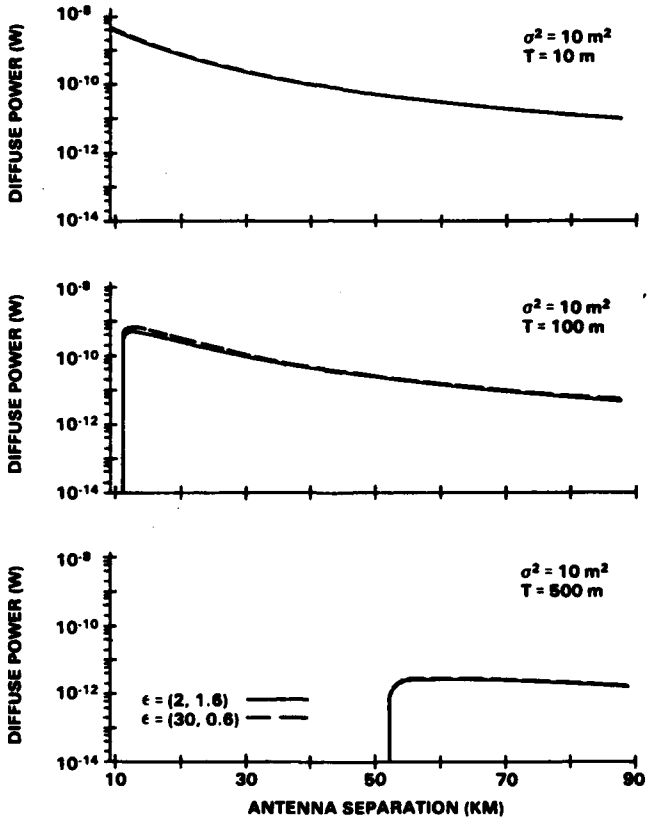

Figure C8. Diffuse Power vs Antenna Separation for a Horizontally Polarized Signal, Standard Surface Model Without Shadowing, at Three Roughness Levels; ——— ϵ = (2, 1.6) and - - - - ϵ = (30, 0.6)

The final area in which we examine differences in behavior as reflected in the two analytical models is that of signal wavelength. The full integration results were discussed in Section 3.4.1. To show differences we compare the results from Figure 15 with corresponding cases for the simple model as shown in Figure C9. Two basic differences can be seen in the effects. For T = 10 m the standard model results in less diffuse power and decreases the relative effect of moisture. At T = 100 m the same type of behavior occurs and in addition there is the cut off of power at short separations.

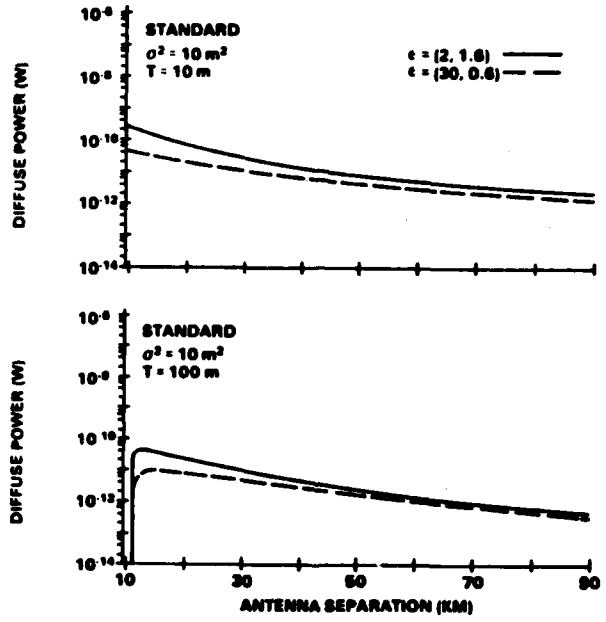

Figure C9. Diffuse Power vs Antenna Separation at a Wavelength of 0.1 M, Standard Surface Model Without Shadowing, at Two Roughness Levels: —— ϵ = (2, 1.6), and - - - - ϵ = (30, 0.6)

This comparison completes the discussion of the sequence of results generated by the two models. The results are included in the text in the summary of conditions examined in the study.

MISSION
of
Rome Air Development Center

RADC plans and executes research, development, test and selected acquisition programs in support of Command, Control Communications and Intelligence (C^3I) activities. Technical and engineering support within areas of technical competence is provided to ESD Program Offices (POs) and other ESD elements. The principal technical mission areas are communications, electromagnetic guidance and control, surveillance of ground and aerospace objects, intelligence data collection and handling, information system technology, solid state sciences, electromagnetics and electronic reliability, maintainability and compatibility.

Printed by
United States Air Force
Hanscom AFB, Mass. 01731